RESULTS & DISCUSSION

3. RESULTS AND DISCUSSION

This study belongs to the most important category of surface active materials, which named cationic surfactants. There are different types of the cationic surfactants, our study concerning only with quaternary ammonium chloride salt (QUATS).

The synthesis of these compounds carried out in two main steps: The first step is preparation of tertiary amine containing hydroxyl group throughout reaction of fatty amine mainly decyl , dodecyl, hexadecyl and octadecylamine with Propylene oxide. The second step is quaternization of tertiary amine with benzyl chloride (Scheme2).

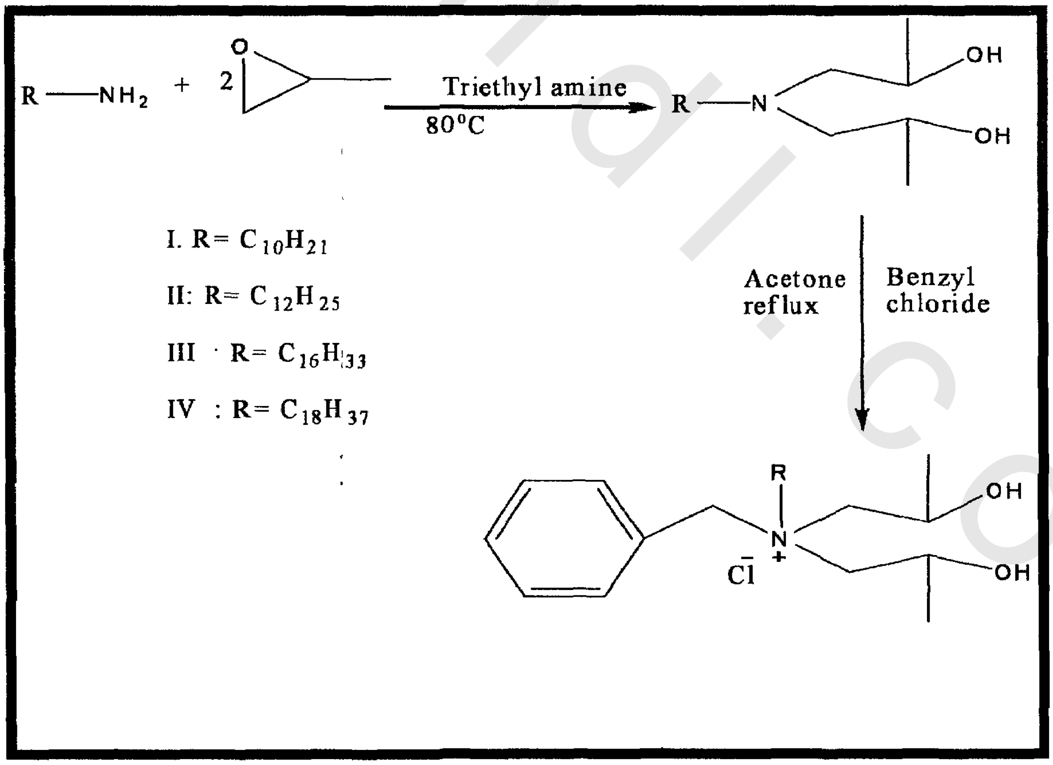

Scheme (2) preparation of cationic surfactant

An example for the chemical structure of the prepared cationic surfactant can be illustrated as following

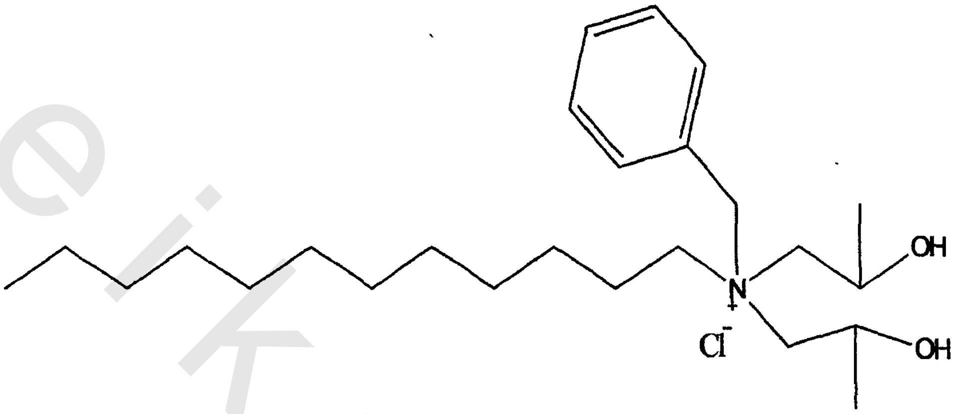

Benzyl-dodecyl-bis-(2-hydroxy-propyl)-ammonium; chloride

3.1. Structure Confirmation of the Prepared Compounds:

The chemical structure of the prepared compounds was confirmed using the following techniques:

3.1.1 Elemental analysis.

The elemental analysis used to determine the percentage of the elements in the compound. Elemental analysis of the prepared compounds are shown in Table (3).

Table (3): The elemental analysis of the prepared cationic surfactants

Compound		I	II	III	IV
C%	Calculated	69.06	70.14	71.94	72.69
	Found	68.22	68.65	70.43	71.18
H%	Calculated	10.58	10.83	11.24	11.41
	Found	10.30	10.12	10.78	10.33
N%	Calculated	3.50	3.27	2.89	2.73
	Found	3.15	2.98	2.54	2.31
Cl%	Calculated	8.86	8.28	7.32	6.92
	Found	8.63	8.03	7.12	6.15

As shown in Table (3), it is clear that the calculated and the found values of microanalysis are very close, this means that these prepared compounds are very pure, and their working out was done by right method.

3.1.2. FTIR Spectroscopy.

The infrared absorption spectra show the general characteristic bands for prepared cationic compounds. The obtained data were given in Table (4) and representative charts in Figures (6-9).

The main absorption bands appear at (2638-2691) cm^{-1} region for all the prepared cationic compounds arises from ammonium ion (N^+),and the absorption bands at (3349-3389) cm^{-1} region for all the prepared compounds arises from hydroxyl group. The very strong bands at (2811.22-2841.56) cm^{-1} region for all the prepared compounds are due mainly to the (-CH-) symmetric stretching vibration. Also, the very strong bands at (2888.83-2928.18) cm^{-1} regions for all the prepared compounds are due mainly to the methylene asymmetric stretching vibration.

Table (4) :Characteristic peaks of the prepared cationic surfactants.

Function group	**wave number cm^{-1}**			
	I	**II**	**III**	**VI**
Hydroxyl group	3389.59	3349.24	3351.26	33389.95
CH$_{aliph}$ Symmetric stretch	2928.18	2921.63	2888.83	2928.18
CH$_{aliph}$ Asymmetric stretch	2841.56	2812.22	2811.02	2840.59
Quaternary salt (R_4N^+)	26638.28	2652.84	2648.62	2691.81
C=C	1741.18	1638.23	1691.54	1659.45
C-N	1139.72	1138.76	1214.93	1135.87
CH$_3$ Bending	1410.67	1376.93	1376.93	1334.03
CH$_2$ asymmetric Bending	1461.76	1410.67	1461.76	1464.67
CH$_2$ multiple(CH$_2$)n Rock	720.46	730.42	725.10	721.247
C-O	1067.47	1079.74	1070.41	1086.37
CH Aromatic	3061.45	3011.54	3021.46	3061.45

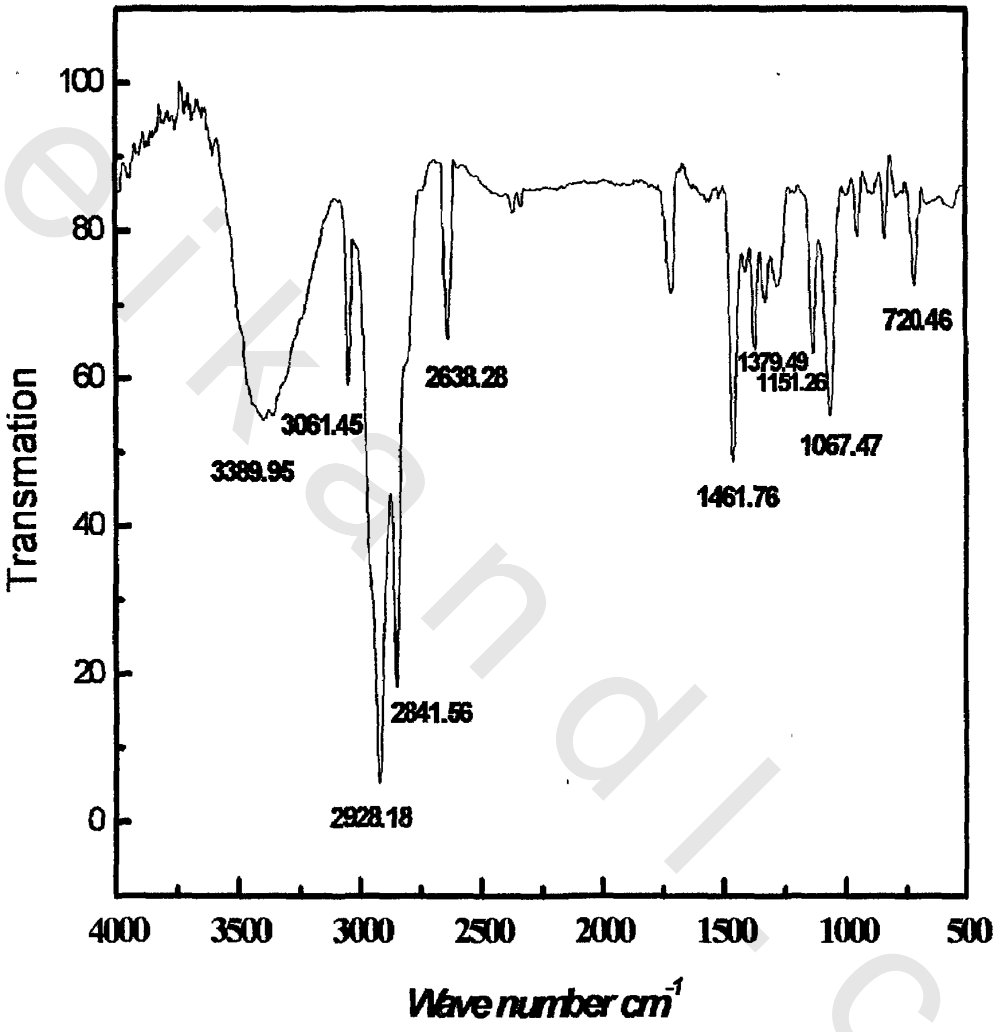

Figure (6) FTIR spectrum of compound (I)

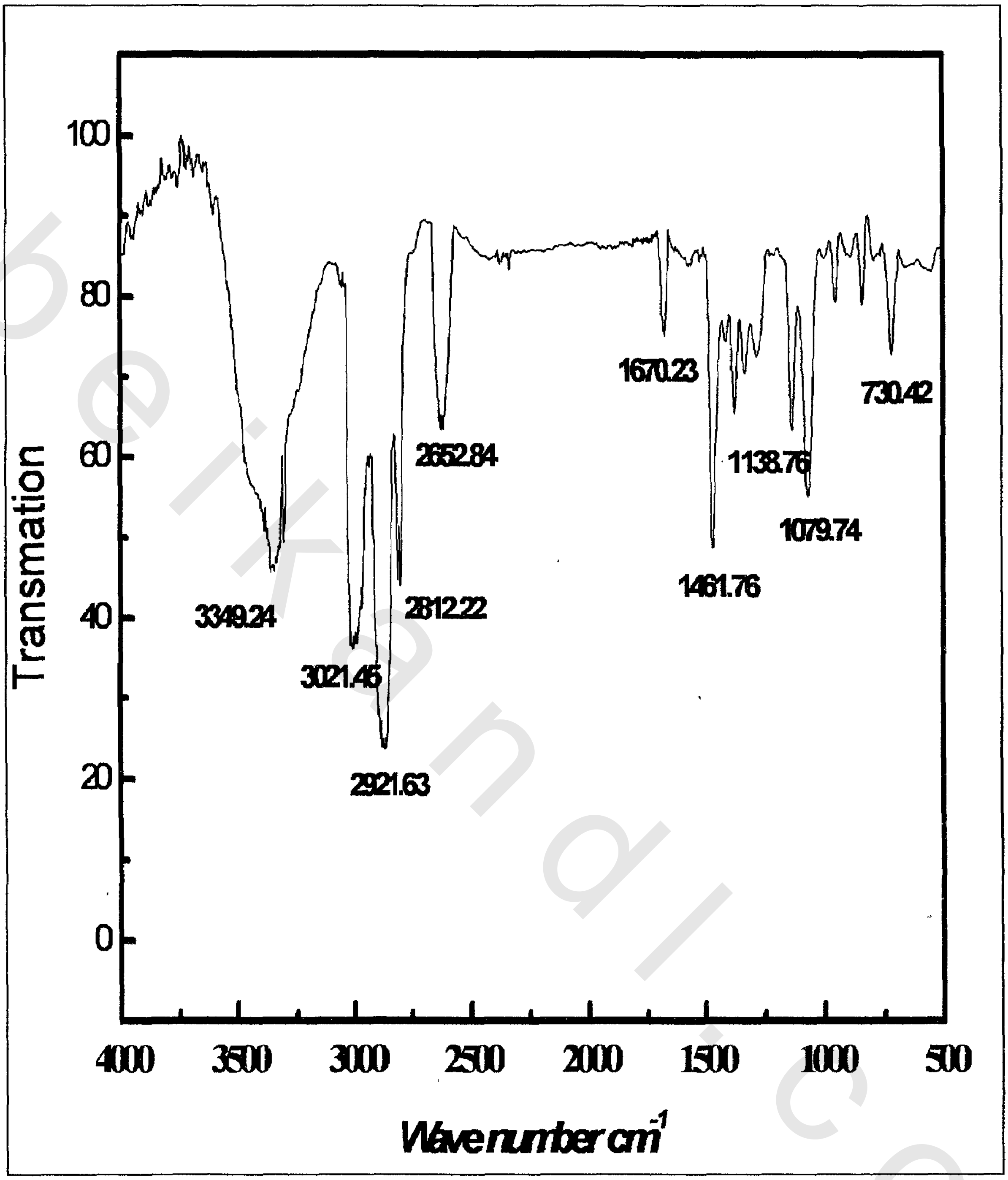

Figure (7) FTIR spectrum of compound (II)

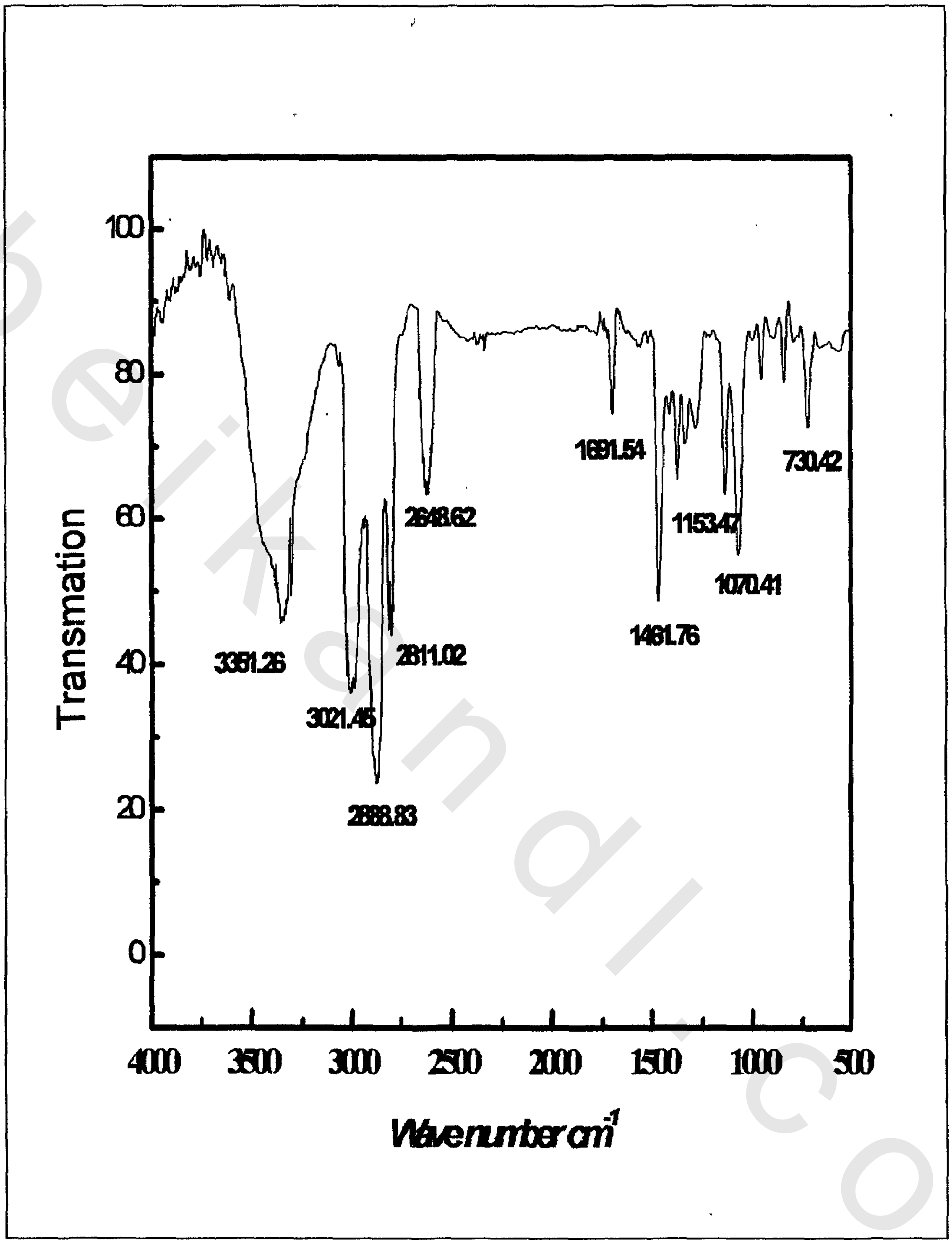

Figure (8) FTIR spectrum of compound (III)

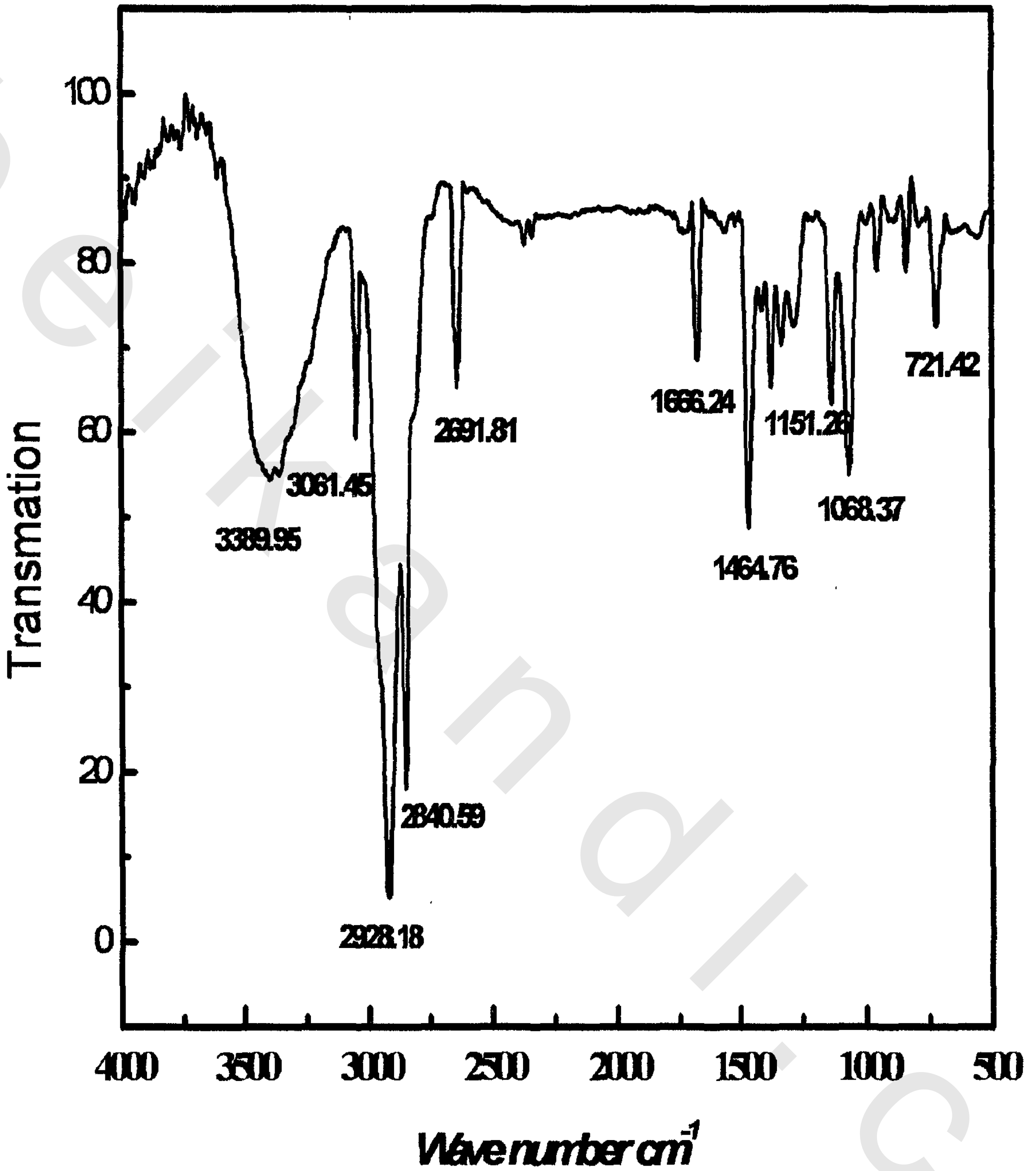

Figure (9) FTIR spectrum of compound (IV)

3.1.3. ^{1}H-NMR Spectroscopy:

The ^{1}H-NMR spectroscopy performed to confirm the number and distribution of hydrogen protons for prepared compounds. The spectrum is shown in Figures (10-13) and is explained as follows:

T he ^{1}H-NMR spectrum data of compound (I) as follows δ=0.848(t,3H,$\underline{CH_3}$-$(CH_2)_9$),δ=1.237(m,2H,$CH_3C\underline{H}_2$-$(CH_2)_8$), δ=1.108 (m,12H,$C\underline{H}_2$ $)_6$ δ=1.688 (m,2H, $C\underline{H}_2$-CH_2N^+) ,δ=3.053 (t,2H,CH_2-$C\underline{H}_2$-N^+);δ=2.504(S,1H,$O\underline{H}$),δ=3.165(S,2H,ph$\underline{CH_2}N^+$) ,δ=3.203(d,2H,$CHC\underline{H}_2N^+$)δ=4.132(S,$CH_3C\underline{H}CH_2N^+$),$\delta$=1.015 (d,3H,$C\underline{H}_3$-CH-$CH_2N^+$),$\delta$=7.504 (m,5H,$CH_2$-$\underline{Ph}$).

The ^{1}H-NMR spectrum data of compound (II) as follows δ=0.848(t,3H,$\underline{CH_3}$-$(CH_2)_9$),δ=1.237(m,2H,$CH_3C\underline{H}_2$-$(CH_2)_{10}$), δ=1.109 (m,12H,$C\underline{H}_2$ $)_8$ δ=1.688 (m,2H, $C\underline{H}_2$-CH_2N^+) ,δ=3.053 (t,2H,CH_2-$C\underline{H}_2$-N^+);δ=2.504(S,1H,$O\underline{H}$),δ=4.513(S,2H,ph$\underline{CH_2}N^+$) ,δ=3.203(d,2H,$CHC\underline{H}_2N^+$)δ=4.132(S,$CH_3C\underline{H}CH_2N^+$),$\delta$=1.015 (d,3H,$C\underline{H}_3$-CH-$CH_2N^+$),$\delta$=7.504 (m,5H,$CH_2$-$\underline{Ph}$).

The ^{1}H-NMR spectrum data of compound (III) as follows δ=0.855(t,3H,$\underline{CH_3}$-$(CH_2)_9$),δ=1.239(m,2H,$CH_3C\underline{H}_2$-$(CH_2)_{14}$), δ=1.120 (m,12H,$C\underline{H}_2$ $)_{12}$ δ=1.668 (m,2H, $C\underline{H}_2$-CH_2N^+) ,δ=3.126 (t,2H,CH_2-$C\underline{H}_2$-N^+);δ=2.505(S,1H,$O\underline{H}$),δ=3.203(S,2H,ph$\underline{CH_2}N^+$) ,δ=3.203(d,2H,$CHC\underline{H}_2N^+$)δ=4.052(S,$CH_3C\underline{H}CH_2N^+$),$\delta$=1.015 (d,3H,$C\underline{H}_3$-CH-$CH_2N^+$),$\delta$=7.504 (m,5H,$CH_2$-$\underline{Ph}$).$\delta$=3.203(2H$CHC\underline{H}_2N^+$)

The ^{1}H-NMR spectrum data of compound (IV) as follows $\delta=0.767(t,3H,\underline{CH_3}\text{-}(CH_2)_9)$,$\delta=1.233(m,2H,CH_3C\underline{H_2}\text{-}(CH_2)_{16})$, $\delta=1.120$ $(m,12H,C\underline{H_2}\ )_{14}$ $\delta=1.679(\ m,2H,\ C\underline{H_2}\text{-}CH_2N^+\ )$,$\delta=3.357$ $(t,2H,CH_2\text{-}C\underline{H_2}\text{-}N^+)$;$\delta=2.506(S,1H,O\underline{H})$,$\delta=3.505(S,2H,ph\underline{CH_2}N^+\ )$,$\delta=3.203(d,2H,CHC\underline{H_2}N^+)$$\delta=4.132(S,CH_3C\underline{H}CH_2N^+)$,$\delta=0.952$ $(d,3H,C\underline{H_3}\text{-}CH\text{-}CH_2N^+)$,$\delta=7.167$ $(m,5H,CH_2\text{-}\underline{Ph})$.

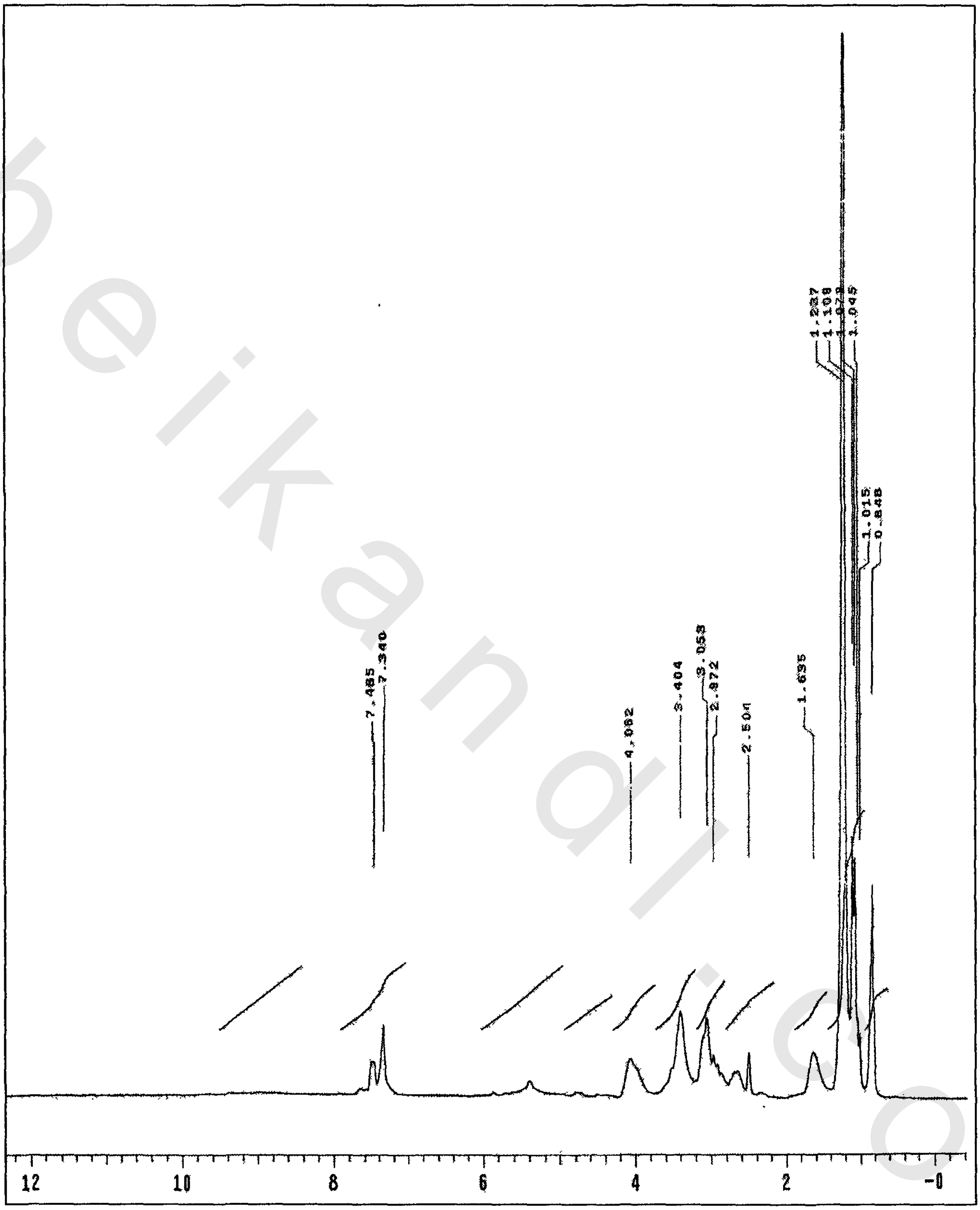

Figure (10)^{1}H-NMR spectrum of compound (I).

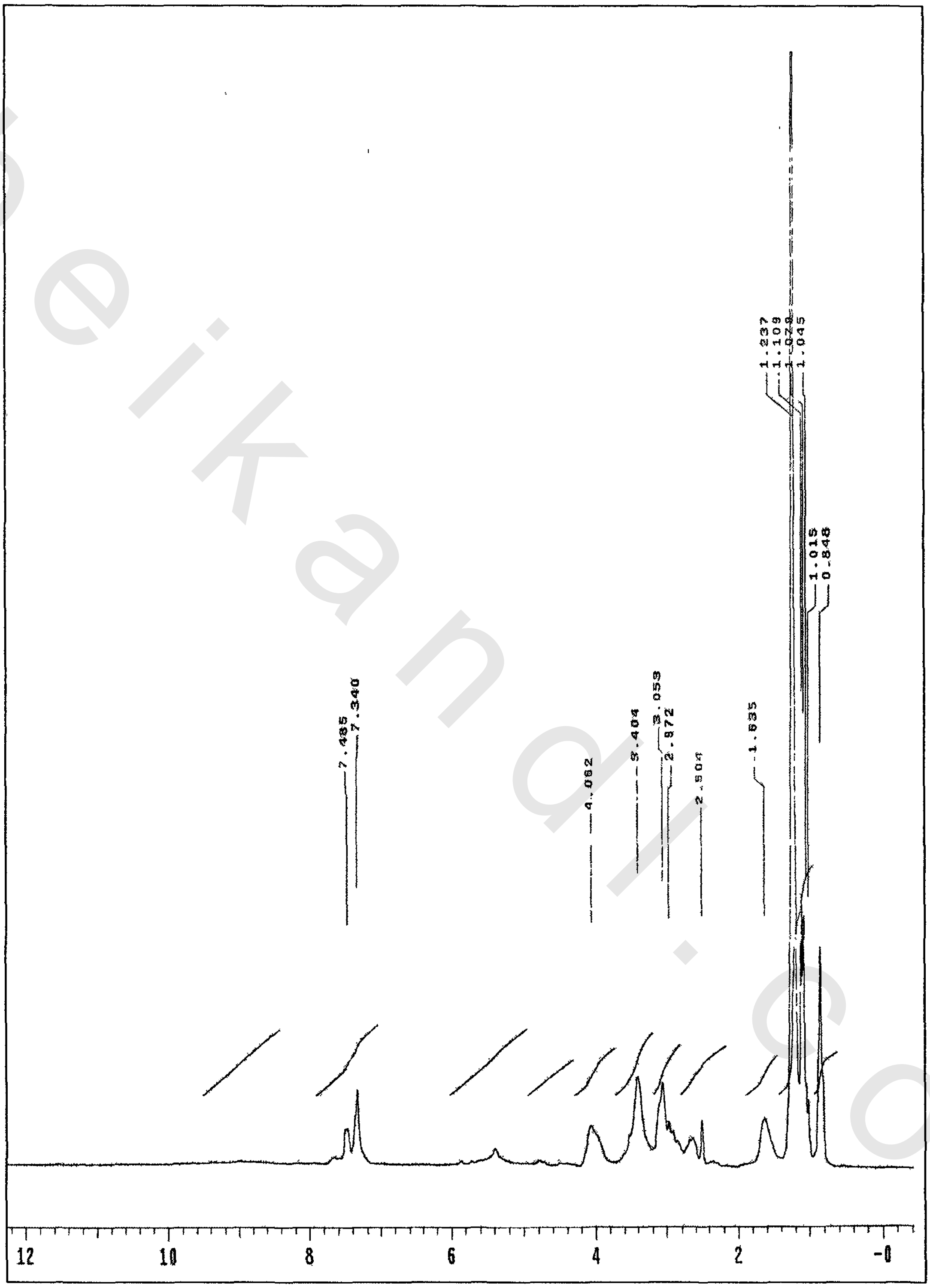

Figure (11) ^{1}H-NMR spectrum of compound (II).

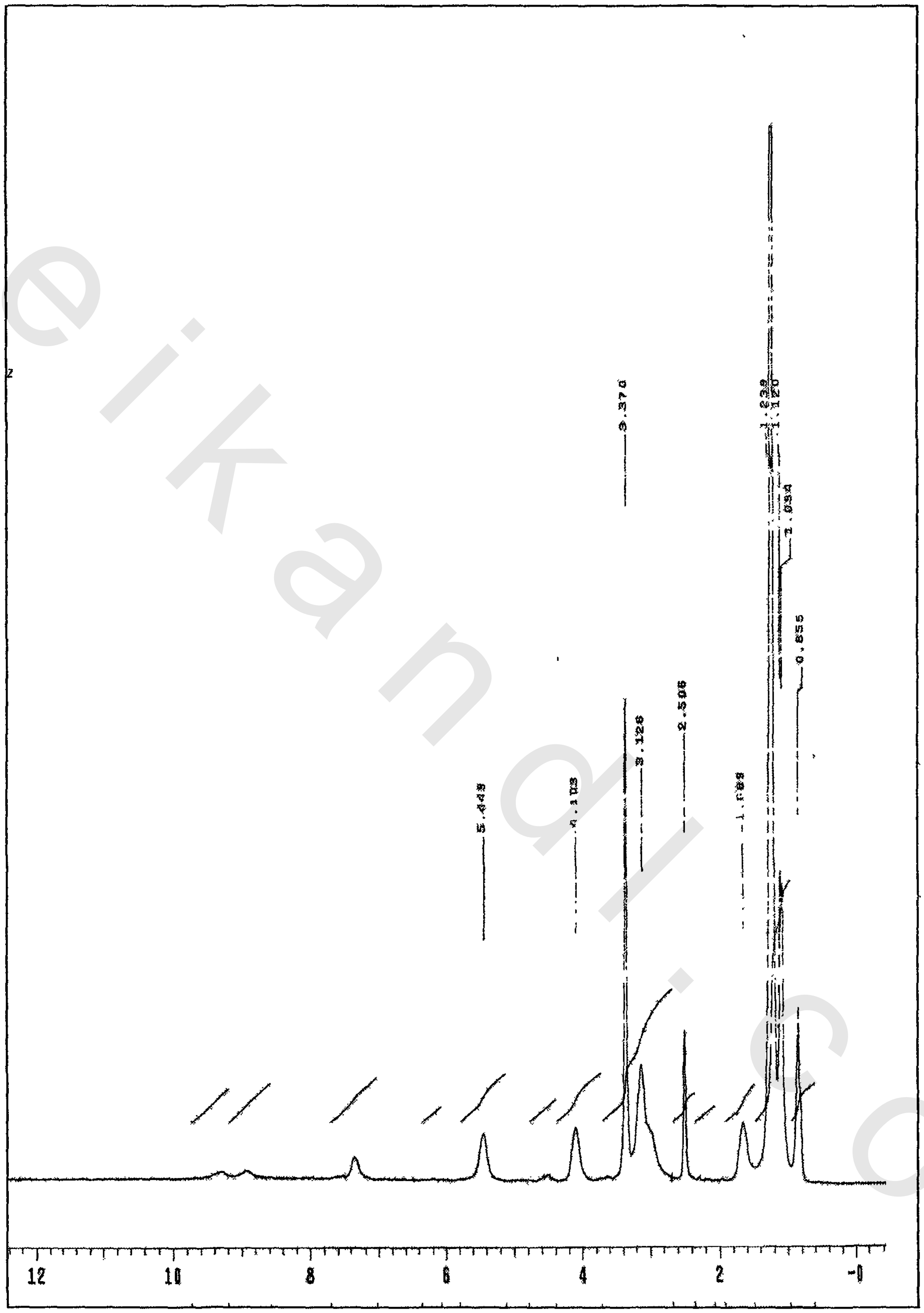

Figure (12) ^{1}H-NMR spectrum of compound (III).

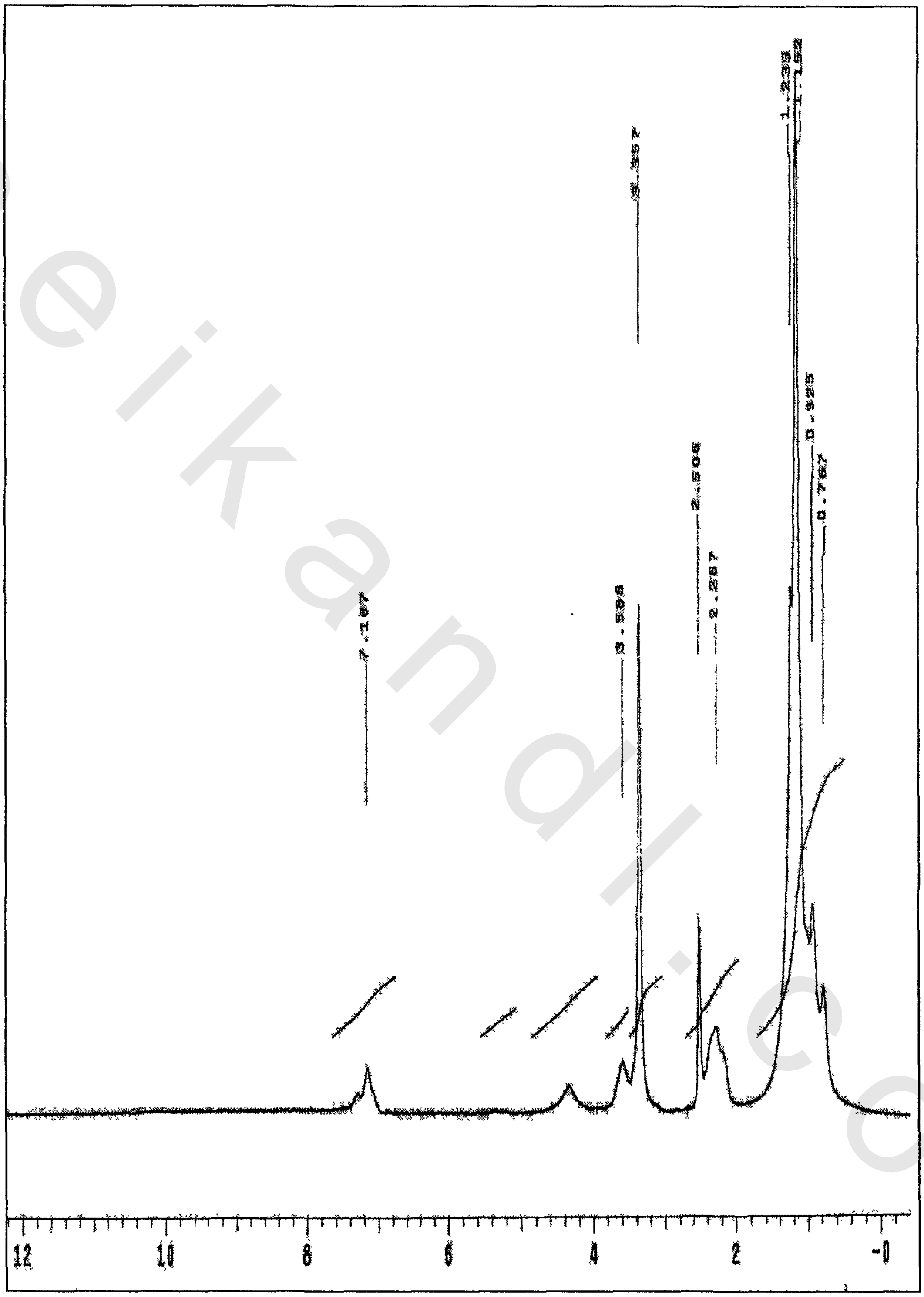

Figure (13) ^{1}H-NMR spectrum of compound (IV).

3.2.The Surface Active Properties of Prepared Compounds

3.2.1. The Surface Tension.

The surface tension is the energy per unit area or the work required to make expansion for the surface against the contracting force. Where the origin of surface tension is the molecule at surface or interface, where these molecules subject to attraction force from molecules in the bulk only, i.e, it was subjected to unequal attraction force from surrounding molecules, this imbalance force pulls the molecules of surface toward interior of liquid leading to contracting the surface area.

The surface tension values were measured for aqueous solution of the prepared cationic surfactants at different concentrations and 25°C. The data are represented as surface tension against concentration of surfactants as shown in Figures (14). It is clear that the surface tension decreases by increasing the concentration of surfactant and also decreases by increasing the hydrophobic chain length at constant concentration. This behavior is due to adsorption of surfactant molecules at a surface. When a surfactant molecule dissolved in the solvent, it distorts the structure of the solvent and therefore increases free energy of the system. These molecules concentrate at interface in a way to minimize the free energy of the system, where the hydrophobic part oriented away from the solvent to avoid the energy unfavorable contact with aqueous media. At the same time the hydrophilic group directed toward the bulk, this adsorption at interface provides an expanding force acting against the normal surface tension [113], Then the surface tension decreased. It is obvious that by increasing the concentration of surfactant, the adsorption at surface will increase as result the surface tension gradually decrease until a stable value is achieved, this lower value of surface tension corresponds the maximum monolayer-level adsorption at air-water interface. Further increase in surfactant concentration above this maximum interfacial adsorption level leads to formation of surfactant aggregation known as micelle. For example the surface tension of compound (I) at concentration of $1x10^{-6}$ M is $62mNm^{-1}$ while at concentration of $5x10^{-4}$ M is 47.2 mNm^{-1}.

Also it was found that by increasing hydrophobic chain length, the surface tension decreases as a result of increasing hydrophobicity. This increase in the free energy of the system leading to adsorption of molecules at surface causing more reduction in surface tension. The surface tension of compound I is 48.2 mNm^{-1} and compound IV is 34.2 mNm^{-1} at concentration of $1x10^{-4}$ M.

3.2.2. The Interfacial Tension.

The interfacial tension was measured between 0.1% aqueous solution of surfactant and light paraffin oil at 25°C; the data were shown in the Table (5). From these data it is clear that by increasing hydrophobic chain length of prepared cationic surfactants, the interfacial values decrease this due to the same reason demonstrated previously in the explanation of surface tension where by increasing hydrophobic chain length of surfactant the free energy of the system increases so molecules tend to adsorb at interface leading to decreasing the interfacial tension.

Table (5): Interfacial tension of prepared compounds

Compound	I	II	III	IV
Interficial tension (mNm^{-1})	14	13	8	6.5

+

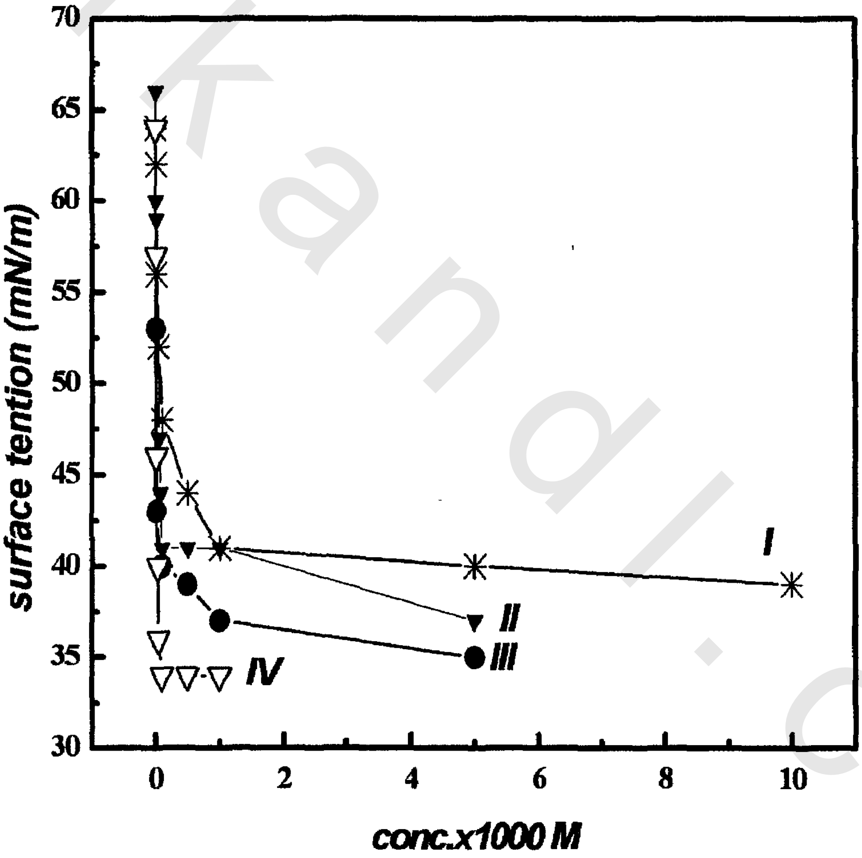

Figure (14) Surface tension against concentration for prepared compounds

3.2.3. The Critical Micelle Concentration (CMC):

Critical micelle concentration values of the prepared cationic surfactants have been obtained graphically by plotting the surface tension (γ) in mNm^{-1} of aqueous solution of the prepared surfactants versus their bulk concentrations in mole/liter at 25°C. The CMC values are listed in Table (6) .The data show that there is a decrease in the CMC of solution with increasing the hydrophobic chain length by increasing hydrophobic chain length; the hydrophobicity increased and solubility decreased thus free energy of the system increased, so surfactant molecules concentrate at the surface in away to minimize free energy of the system. However there is another mean for reducing free energy that by aggregation of the surface-active agent molecules into clusters (micelles), where the hydrophilic group are directed toward the solvent while the hydrophobic chain are directed toward the interior of the micelle in away to avoid energically unfavorable contact with the aqueous media, thereby reducing the free energy of the system. So by increasing hydrophobic chain length, the tendency of the surfactant molecule to form micelle increased and this leads to decrease the CMC.

Table (6): CMC of prepared compounds

Compound	I	II	III	IV
CMCX10^{-4}(M)	3.60	1.80	1.40	1.04

63.3. Evaluation of Prepared Compounds as Corrosion Inhibitors.

Corrosion protection of steel in acidic media is of great important both for industrial facilities and theoretical aspects. The use of inhibitor is one of the most practical methods for protection of steel against corrosion in acidic media. Among all inhibitors, the most important are the organic ones, also called adsorption inhibitors. They control corrosion, acting over the anodic or the cathodic surface or both. Most commercial acid inhibitors are organic compounds containing hetero atoms such as nitrogen, oxygen, sulfur, phosphor atoms, by which the inhibitor molecules are adsorbed on the metal surface in acidic media, thus resulting adsorption film acts as a barrier separating the metal from the corrosive medium and blocks the active sites. As a representative type of these organic inhibitors, quaternary ammonium salts have been demonstrated to be highly cost-effective and used widely in various industrial processing for preventing corrosion of iron and steel in acidic media.

Three different techniques used in this work to determine the corrosion rate and corrosion inhibition efficiency.

3.3.1.Wight Loss Technique.

The corrosion rate of carbon steel sheet was calculated from the following equation:

$$CR = W/At \quad (21)$$

Where CR is the corrosion rate, W is the average weight loss of three parallel carbon steel samples in milligram, A is the total area of the specimen by cm^2 and t is immersion time by hour. The corrosion rate data of carbon steel sample with and without addition of prepared corrosion inhibitors in corrosive medium 1M H_2SO_4 at various temperatures are shown in Tables (7-9). Table (7) represents the corrosion rat values for all prepared inhibitors at 298 K. Form the data in this table it is clear that the corrosion rate values in mg $cm^{-2}h^{-1}$ decrease with increasing inhibitor concentrations taking compound (I) as example the corrosion rate value is 5.22 (mg $cm^{-2}h^{-1}$) for blank solution then by addition of the inhibitor the corrosion rate value decreased gradually by increasing the concentration of the inhibitor reache to value 0.40 mg $cm^{-2}h^{-1}$ at concentration of $5x10^{-3}$ M of compound (I). This behavior is the same for all prepared inhibitors (I, II, IV).from same table it is clear that the lowest corrosion rate is 0.07(gm $cm^{-2}h^{-1}$) at concentration of $5x10^{-3}$ Mof compound (II).

Also the influence of temperature on corrosion rat in absence and in presence of prepared compounds has been discussed in Tables (7-9). These tables show that the corrosion rate values increase by increasing the temperature the value of corrosion rate in blank solution was (5.22, 6.91, and 8.93 mg $cm^{-2}h^{-1}$) at temperature 298, 308 and 318 K, respectively. This increase in corrosion rate due to the increase in temperature enhance the rate of (H^+) diffusion to the metal surface beside the ionic mobility. The effect of prepared compounds on corrosion rate at these temperatures is also studied. It is clear that the corrosion rate decreased gradually by increasing concentration of the added compound. These results confirm that each prepared compound acts as an efficient inhibitor in the range of temperature stuied.

Table (7): Corrosion rate of carbon steel with and without addition of prepared compounds as corrosion inhibitors in 1M H_2SO_4 at 298K

Conc. (M)x10^5	Corrosion Rate(mg $cm^{-2}h^{-1}$)			
	I	II	III	IV
0.00	5.22	5.22	5.22	5.22
1.00	3.60	3.21	3.75	2.80
5.00	2.53	2.29	2.58	1.73
10.0	2.14	0.48	1.67	1.55
50.0	1.36	0.22	1.18	1.27
100	0.84	0.16	0.90	1.18
500	0.40	0.07	0.27	0.82

Table (8): Corrosion rate of carbon steel with and without addition of prepared compounds as corrosion inhibitors in 1M H_2SO_4 at 308K

Conc. (M)x10^5	Corrosion Rate (mg $cm^{-2}h^{-1}$)			
	I	II	III	IV
0.00	6.91	6.91	6.91	6.91
1.00	5.27	5.82	6.06	4.31
5.00	4.38	4.91	4.59	2.82
10.0	3.30	2.14	2.94	2.30
50.0	2.67	0.99	1.44	2.12
100	1.98	0.77	0.82	1.78
500	0.59	0.39	0.44	1.34

Table (9): Corrosion rate of carbon steel with and without addition of prepared compounds as corrosion inhibitors in 1M H_2SO_4 at 318K

Conc.(M)x10^5	Corrosion Rate(mg $cm^{-2}h^{-1}$)			
	I	II	III	IV
0.00	8.93	8.93	8.93	8.93
1.00	6.38	6.10	7.25	8.33
5.00	5.76	5.35	5.85	6.57
10.0	4.21	2.04	4.14	4.73
50.0	3.27	1.28	3.48	2.49
100	2.26	1.08	3.08	2.36
500	1.31	0.55	1.08	2.27

3.3.1.1. Efficiency of prepared compounds as corrosion inhibitors.

The inhibition efficiency (η %) of an inhibitor was calculated from the following equation:

$$\eta \% = (CR-CR^{\backslash})/ CR \times 100 \qquad (22)$$

Where **CR** and **CR**$^{\backslash}$ were corrosion rate values of carbon steel in absence and presence of inhibitor, respectively

The inhibition efficiency of the organic compounds depends on many factors including the number of adsorption sites and their charge density, molecular size, mode of interaction with the metal surface and formation of metallic complexes [114]. The inhibition of a corrosion process by addition of surfactants may take place through two effects, namely blocking and hydrophobic effects. The former occurs when the inhibitor molecule is adsorbed on the metal surface through the adsorption centers in the molecule. In the investigated surfactants there is (N^+) group and two oxygen atoms which can act as adsorption centers in the molecule. Adsorption of cationic inhibitor prevents contact between the steel surface and the acid solution. It exists at the interface and attaches or adsorb to the metal surface. The adsorption takes place by head group (N^+) and tail group (hydrocarbon chain) of each molecule forming barrier film. The hydrophilic group (N^+) with its counter chloride ion is adsorbed onto the steel surface by electrostatic attraction while the hydrophobic covered the steel. The adsorption takes place by dipole induced interaction with the steel surface as a result of π electron polarization. At same time, immersion of carbon steel in 1M H_2SO_4 showed an adsorption of the sulfate ions on the steel surface leading to the availability of more negative sites on the metal surface. As the result, hydrophilic group prefer adsorptions on the steel surface [115]. The second effect of inhibitors is hydrophobing the interface by surface active compounds to inhibit charge and mass transfer. Surfactants have a characteristic structure consisting of a structural group that has very little attraction for the solvent, known as a hydrophobic group, together with a polar head. When the surfactant is dissolved in water, the presence of the hydrophobic group in the solvent causes a distortion of the solvent liquid structure, increasing the free energy of the system. As compromise, the surfactant concentrates at the interface because their thermodynamically best arrangement is possible. At the metal solution interface the surfactant molecules orientate their polar heads toward the metal and are adsorbed on its surface. The hydrophobic part is oriented away into the solution, repelling thus, the aqueous fluid. Under such conditions a diffusion barrier to chemical and/or electrochemical attack of the solution on the metal surface is established. The inhibiting effect increases with an increase of surfactant concentration [116]. At low surfactant concentration the adsorption takes place by horizontal adsorpation to hydrophobic region. This adsorption is a competitive one because the inhibitor displaces progressively the water molecules and other ions adsorbed. When surfactant concentration increases, a perpendicular adsorption takes place as a result of an inter-hydrophobic chain interaction [117].

Inspection of the data in Tables (10-13) and Figures (15-18) it is obvious the inhibition efficiency of prepared inhibitors increases rapidly at first with increasing concentration of prepared inhibitor until certain concentration, then inhibition efficiency increase slightly. As show in compound (II), Table (13) the inhibition efficiency increase rapidly form 38.50% at concentration $1x10^{-5}$ M to 90.78% at concentration $1x10^{-4}$ M after that the efficiency slightly increase with increasing the concentration.

For comparing the prepared compounds as corrosion inhibitors it was found that the efficiency of these compounds increase in the order IV <I < III< II. This order is the same as that of the inhibition efficiency of the prepared inhibitor. The inhibition of compounds (IV, III) is less than predicted that could be refer to the geometrical conformation occurred in the alkyl chain. This conformation (coiling) causes a compactness in IV and III molecules which decreases their actual volume [118].

Table (10): Inhibition efficiency of compound (I) in 1M H_2SO_4 for the carbon steel sample at different temperatures and concentrations

T(K)	Conc. of inhibitor $[I]\times10^5$(M)	-log [I]	η (%)
298	1.00	5.00	30.99
	5.00	4.30	51.40
	10.0	4.00	58.97
	50.0	3.30	73.92
	100	3.00	83.94
	500	2.30	92.29
308	1.00	5.00	23.78
	5.00	4.30	36.70
	10.0	4.00	52.29
	50.0	3.30	61.32
	100	3.00	71.27
	500	2.30	91.37
318	1.00	5.00	28.59
	5.00	4.30	35.58
	10.0	4.00	52.89
	50.0	3.30	63.44
	100	3.00	74.73
	500	2.30	85.39

Table (11): Inhibition efficiency of compound (II) in 1M H_2SO_4 for the carbon steel sample at different temperatures and concentrations

T(K)	Conc. of inhibitor [I]x105(M)	-log [I]	η (%)
298	1.00	5.00	38.51
	5.00	4.30	56.14
	10.0	4.00	90.78
	50.0	3.30	95.85
	100	3.00	96.89
	500	2.30	98.65
308	1.00	5.00	15.77
	5.00	4.30	28.94
	10.0	4.00	68.97
	50.0	3.30	85.68
	100	3.00	88.82
	500	2.30	94.32
318	1.00	5.00	31.74
	5.00	4.30	40.12
	10.0	4.00	77.22
	50.0	3.30	85.72
	100	3.00	87.89
	500	2.30	93.86

Table (12): Inhibition efficiency of compound (III) in 1M H_2SO_4 for the carbon steel sample at different temperatures and concentrations

T(K)	Conc. of inhibitor $[I]x10^5(M)$	-log [I]	η (%)
298	1.00	5.00	28.16
	5.00	4.30	50.52
	10.0	4.00	68.02
	50.0	3.30	77.42
	100	3.00	82.79
	500	2.30	94.82
308	1.00	5.00	12.32
	5.00	4.30	33.55
	10.0	4.00	57.44
	50.0	3.30	79.24
	100	3.00	88.13
	500	2.30	93.70
318	1.00	5.00	18.81
	5.00	4.30	34.79
	10.0	4.00	53.66
	50.0	3.30	61.05
	100	3.00	65.58
	500	2.30	87.89

Table (13): Inhibition efficiency of compound (IV) in 1M H_2SO_4 for the carbon steel sample at different temperatures and concentrations

T(K)	Conc. of inhibitor $[I]x10^5(M)$	-log [I]	η (%)
298	1.00	5.00	46.39
	5.00	4.30	66.73
	10.0	4.00	70.26
	50.0	3.30	75.68
	100	3.00	77.36
	500	2.30	84.35
308	1.00	5.00	37.61
	5.00	4.30	59.11
	10.0	4.00	66.72
	50.0	3.30	69.35
	100	3.00	74.25
	500	2.30	80.54
318	1.00	5.00	6.81
	5.00	4.30	26.49
	10.0	4.00	47.10
	50.0	3.30	72.11
	100	3.00	73.59
	500	2.30	74.64

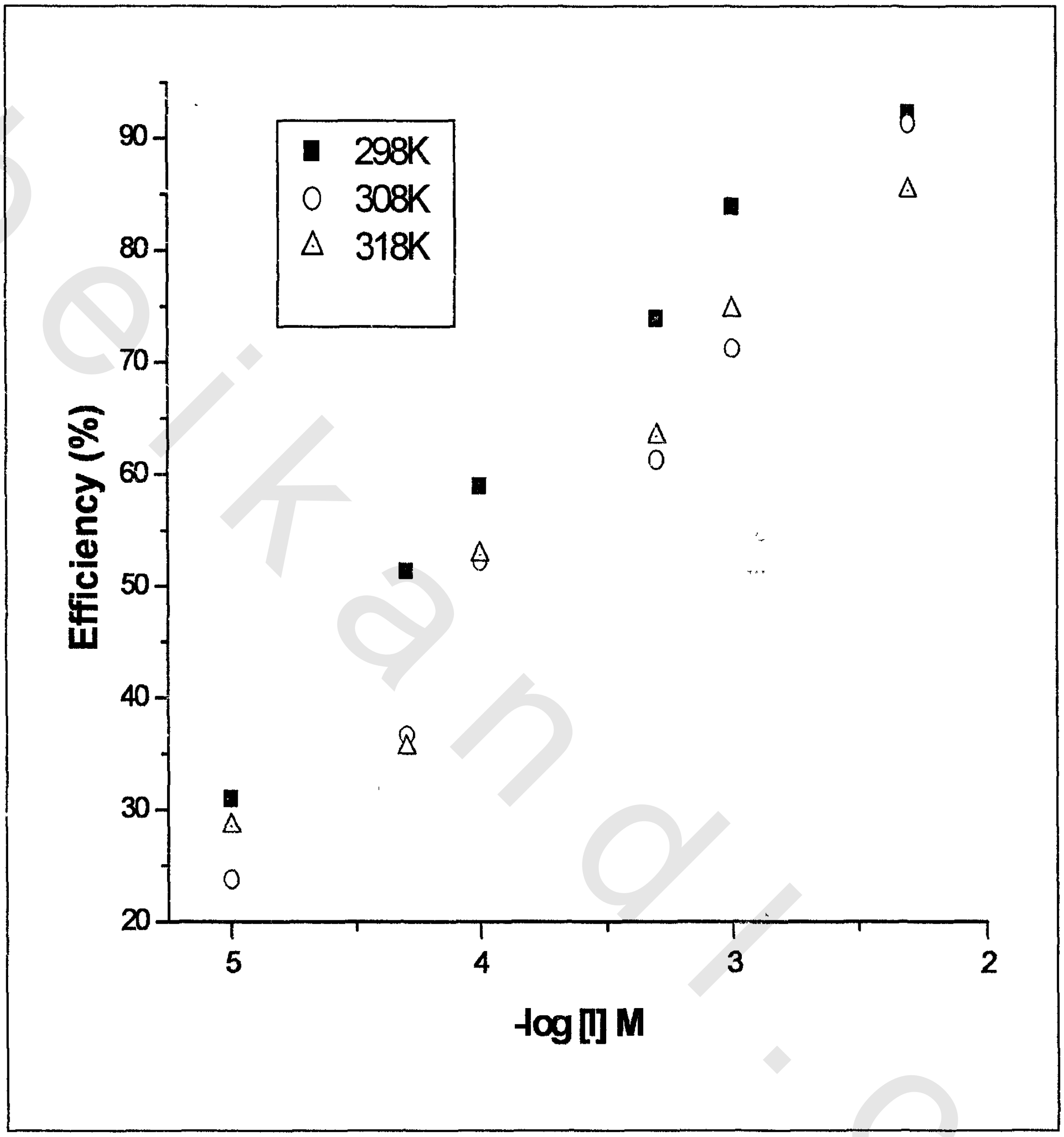

Figure (15): The relation between inhibition efficiency and log [I] of compound (I) in 1 M H_2SO_4 for the carbon steel sample at 298,308 and 318 K.

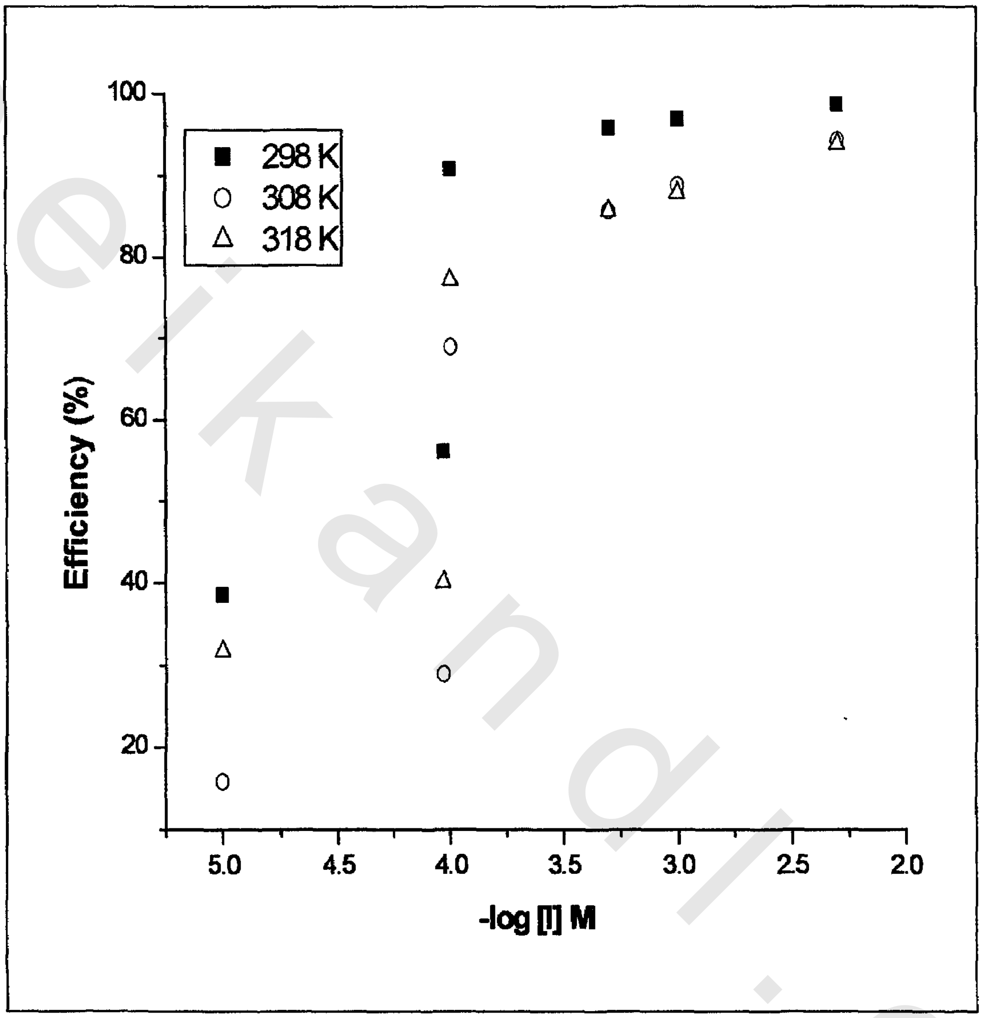

Figure (16): The relation between inhibition efficiency and log [I] of compound (II) in 1 M H_2SO_4 for the carbon steel sample at 298,308 and318K.

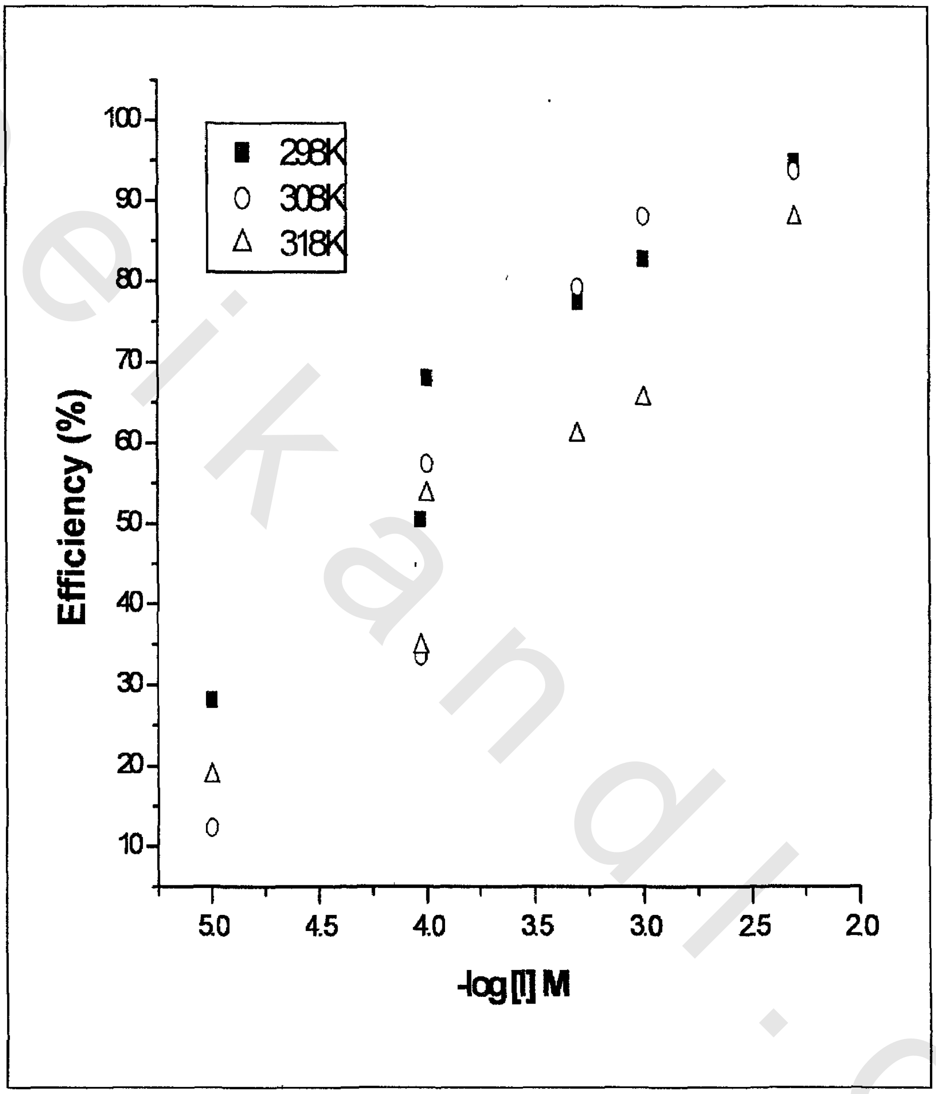

Figure (17): The relation between inhibition efficiency and log [I] of compound (III) in 1 M H_2SO_4 for the carbon steel sample at 298, 308 and318K.

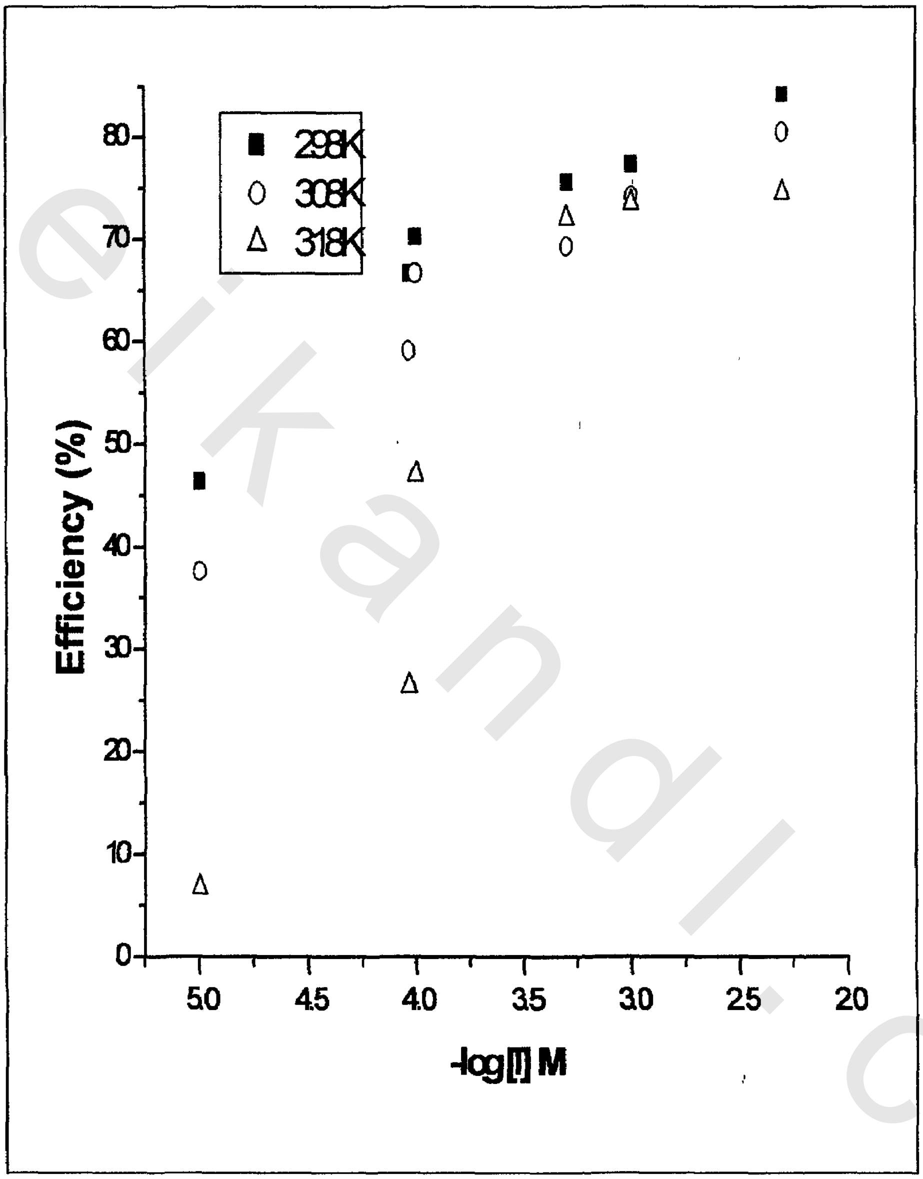

Figure (18): The relation between inhibition efficiency and log [I] of compound (IV) in 1 M H_2SO_4 for the carbon steel sample at 298, 308 and 318K.

3.3.1.2. Activation Energy.

The activation energy, E_a, for the corrosion of the carbon steel sample in 1 M H_2SO_4 solution in absence and presence of different concentrations of prepared inhibitors was calculated from Arrhenius equation (23):

$$\mathbf{CR = A \exp(-E_a / RT)} \quad \mathbf{(23)}$$

Where "A" is the frequency factor, "R" is the universal gas constant, and "T" is the absolute temperature.

A plot of logarithm of corrosion rate (log CR) versus reciprocal of absolute temperature (1/ T) will gives straight line with slope ($-E_a$ / 2.303R). From inspection of the data in Tables (14-17) for the carbon steel sample in absence of inhibitor, showed a value of E_a less than in presence of inhibitors, and that Ea values increased by increasing the concentration of inhibitors. It is obvious that concentration of inhibitors [I] is playing a role in increasing the activation energy value, thereby indicating a more efficient inhibiting effect. These results are according with the reported studies [1119, 120]. The increase of Ea in presence of the inhibitors indicates the physical adsorption or weak chemical bonding between the compounds molecules and the steel surface [121].

Table (14): Activation energy of carbon steel sample in 1M H_2SO_4 of compound (I) at different concentrations

Conc. of inhibitor [I] (M)x10^5	T(K)	-log (C R)	E_a (kJmol^{-1})
0.00	298 308 318	0.72 0.84 0.95	57.89
1.00	298 308 318	0.56 0.72 0.80	61.78
5.00	298 308 318	0.40 0.64 0.76	88.66
10.0	298 308 318	0.33 0.52 0.62	72.95
50.0	298 308 318	0.13 0.43 0.51	94.76
100	298 308 318	0.08 0.30 0.35	107.51
500	298 308 318	0.40 0.22 0.12	126.24

Table (15): Activation energy of carbon steel sample in 1M H_2SO_4 of compound (II) at different concentrations

Conc. of inhibitor [I] (M)x10^5	T (K)	-log (C R)	E_a (kJmol^{-1})
0.00	298 308 318	0.72 0.84 0.95	57.89
1.00	298 308 318	0.51 0.77 0.79	69.74
5.00	298 308 318	0.36 0.69 0.73	92.17
10.0	298 308 318	0.32 0.33 0.31	157.07
50.0	298 308 318	0.66 0.00 0.11	192.26
100	298 308 318	0.79 0.11 0.03	205.51
500	298 308 318	1.15 0.41 0.26	222.63

Table (16): Activation energy of carbon steel sample in 1M H_2SO_4 of compound (III) at different concentrations

Conc. of inhibitor [I] (M)x10^5	T (K)	-log (C R)	E_a (kJmol^{-1})
0.00	298	0.72	57.89
	308	0.84	
	318	0.95	
1.00	298	0.57	71.38
	308	0.78	
	318	0.86	
5.00	298	0.41	87.97
	308	0.66	
	318	0.77	
10.0	298	0.22	98.05
	308	0.47	
	318	0.62	
50.0	298	0.07	115.76
	308	0.16	
	318	0.54	
100	298	0.05	130.39
	308	0.09	
	318	0.49	
500	298	0.57	148.17
	308	0.36	
	318	0.03	

Table (17): Activation energy of carbon steel sample in 1M H_2SO_4 of compound (IV) at different concentrations

Conc. of inhibitor [I] (M)x10^5	T (K)	-log (C R)	E_a (kJmol^{-1})
0.00	298	0.72	57.89
	308	0.84	
	318	0.95	
1.00	298	0.45	117.09
	308	0.63	
	318	0.92	
5.00	298	0.24	142.79
	308	0.45	
	318	0.82	
10.0	298	6.76	118.95
	308	6.68	
	318	6.27	
50.0	298	6.85	73.01
	308	6.62	
	318	6.55	
100	298	6.88	108.77
	308	6.70	
	318	6.44	
500	298	6.84	61.20
	308	6.82	
	318	6.59	

3.3.1.3. Adsorption Isotherm.

The prepared compounds inhibit the corrosion process by adsorption on metal surface. Theoretically, the adsorption process in which an inhibitor species, in the aqueous phase, substitutes an "x" number of water molecules adsorbed on the metal surface [123], according to the following equation (24):

$$I_{aq} + x\,H_2O \longrightarrow I_s + x\,H_2O_{aq} \qquad (24)$$

Where "x" is known as the size ratio, and simply equals the number of adsorbed water molecules replaced by a single inhibitor molecule.

The adsorption depends on the structure of the inhibitor, the type of the metal and the nature of its surface, the nature of the corrosion medium, the temperature, and the electrochemical potential of the metal – solution interface.

The adsorption provides information about the interaction among the adsorbed species themselves as well as their interaction with the charged surface. The mathematical relationship for the adsorption isotherms suggested fitting the experimental data of the present work is Langmuir model.

Langmuir Model.

The simple equation is that of Langmuir [124,125]:

$$\theta / 1 - \theta = K_{ads}\,[I] \qquad (25)$$

Where "K_{ads}" is the equilibrium constant of the adsorption reaction, [I] is the inhibitor concentration in the bulk of the solution, and "θ" is the surface coverage.

The surface coverage, θ, is the fraction of surface covered by the inhibitor molecules. It was calculated from the following equation:

$$\theta = 1-(CR^{\backslash} / CR) \quad (26)$$

Where $CR^{\backslash}$ and CR are the corrosion rates in the presence and absence of the inhibitor, respectively.

The values of "θ" for the carbon steel sample in 1 M H_2SO_4 in different concentrations of prepared compounds at different temperatures were determined.

Tables (18-21) show the values of (θ / 1− θ) and K_{ads} for all prepared compounds.

Figures (19-22) show the relation between (θ / 1− θ) and [I] (Langmuir adsorption plots) for adsorption of prepared compounds on the surface of carbon steel sample in 1 M H_2SO_4 solution.

The above relation is straight line, which indicates that the Langmuir isotherm model is valid for this system. Langmuir's isotherm applied for ideal case of a physical and chemical adsorption on a smooth surface with no interaction between the adsorbed molecules.

Table (18): The adsorption constant (K_{ads}) of compound (I) 1 M H_2SO_4 different temperatures

T(K)	Conc. of inhibitor [I]x10^5M	θ /1-θ	K_{ads}
298	1.00	0.45	2183.29
	5.00	1.06	
	10.0	1.43	
	50.0	2.83	
	100	5.23	
	500	11.97	
308	1.00	0.31	2008.48
	5.00	0.58	
	10.0	1.09	
	50.0	1.59	
	100	2.48	
	500	10.59	
318	1.00	0.40	1016.84
	5.00	0.55	
	10.0	1.12	
	50.0	1.73	
	100	2.95	
	500	5.84	

Table (19): The adsorption constant (K_{ads}) of compound (II) 1 M H_2SO_4 different temperatures

T(K)	Conc. of inhibitor $[I]x10^5M$	θ /1-θ	K_{ads}
298	1.00	0.62	13519.31
	5.00	1.28	
	10.0	9.85	
	50.0	23.08	
	100	31.12	
	500	73.16	
308	1.00	0.19	3031.04
	5.00	0.41	
	10.0	2.22	
	50.0	5.98	
	100	7.95	
	500	16.61	
318	1.00	0.47	2668.62
	5.00	0.67	
	10.0	3.39	
	50.0	6.01	
	100	7.25	
	500	15.29	

Table (20): The adsorption constant (K_{ads}) of compound (III) 1 M H_2SO_4 different temperatures

T(K)	Conc. of inhibitor $[I]\times10^5$M	θ /1-θ	K_{ads}
298	1.00	0.39	3440.18
	5.00	1.02	
	10.0	2.12	
	50.0	3.43	
	100	4.81	
	500	18.30	
308	1.00	0.14	2789.38
	5.00	0.50	
	10.0	1.35	
	50.0	3.82	
	100	7.43	
	500	14.86	
318	1.00	0.23	1328.26
	5.00	0.53	
	10.0	1.16	
	50.0	1.57	
	100	1.91	
	500	7.25	

Table (21): The adsorption constant (K_{ads}) of compound (IV) 1 M H_2SO_4 different temperatures

T (K)	Conc. of inhibitor $[I] x 10^5 M$	θ /1-θ	K_{ads}
298	1.00	0.87	701.21
	5.00	2.01	
	10.0	2.36	
	50.0	3.11	
	100	3.41	
	500	5.39	
308	1.00	0.60	539.82
	5.00	1.45	
	10.0	2.00	
	50.0	2.26	
	100	2.88	
	500	4.14	
318	1.00	0.07	434.63
	5.00	0.36	
	10.0	0.89	
	50.0	2.58	
	100	2.78	
	500	2.94	

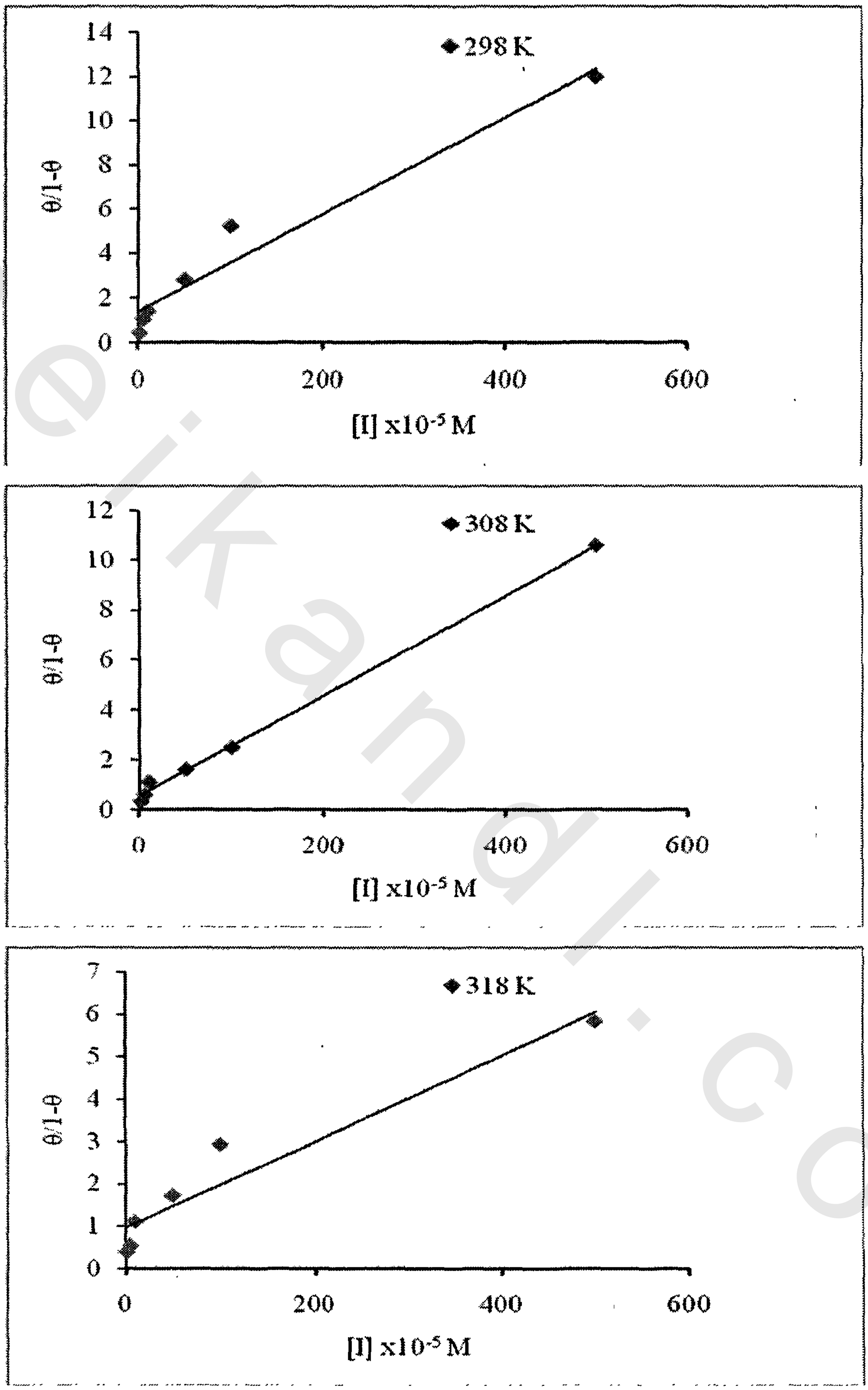

Figure (19): Relation between (θ / 1– θ) and concentration of compound (I).

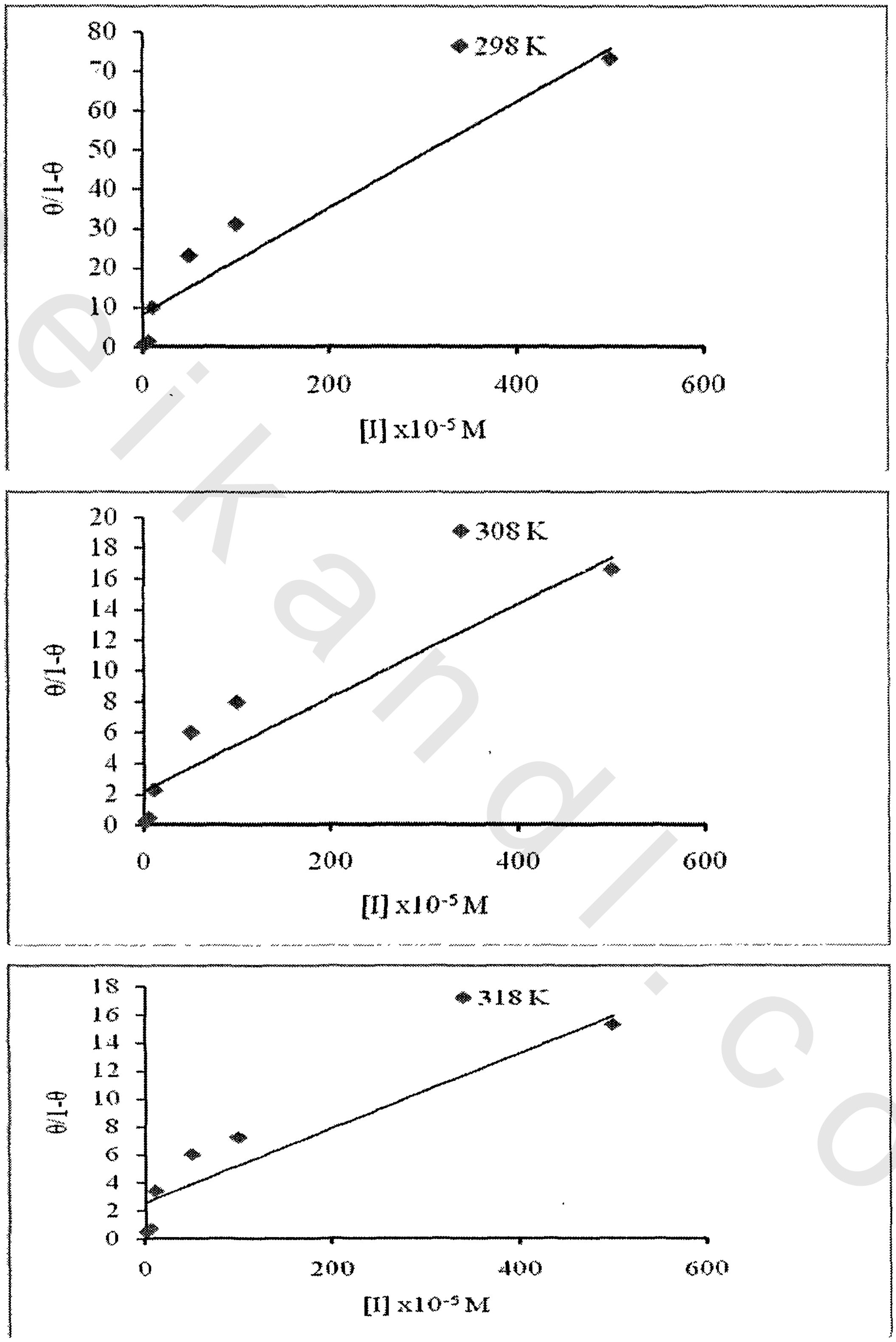

Figure (20): Relation between (θ / 1– θ) and concentration of compound (II).

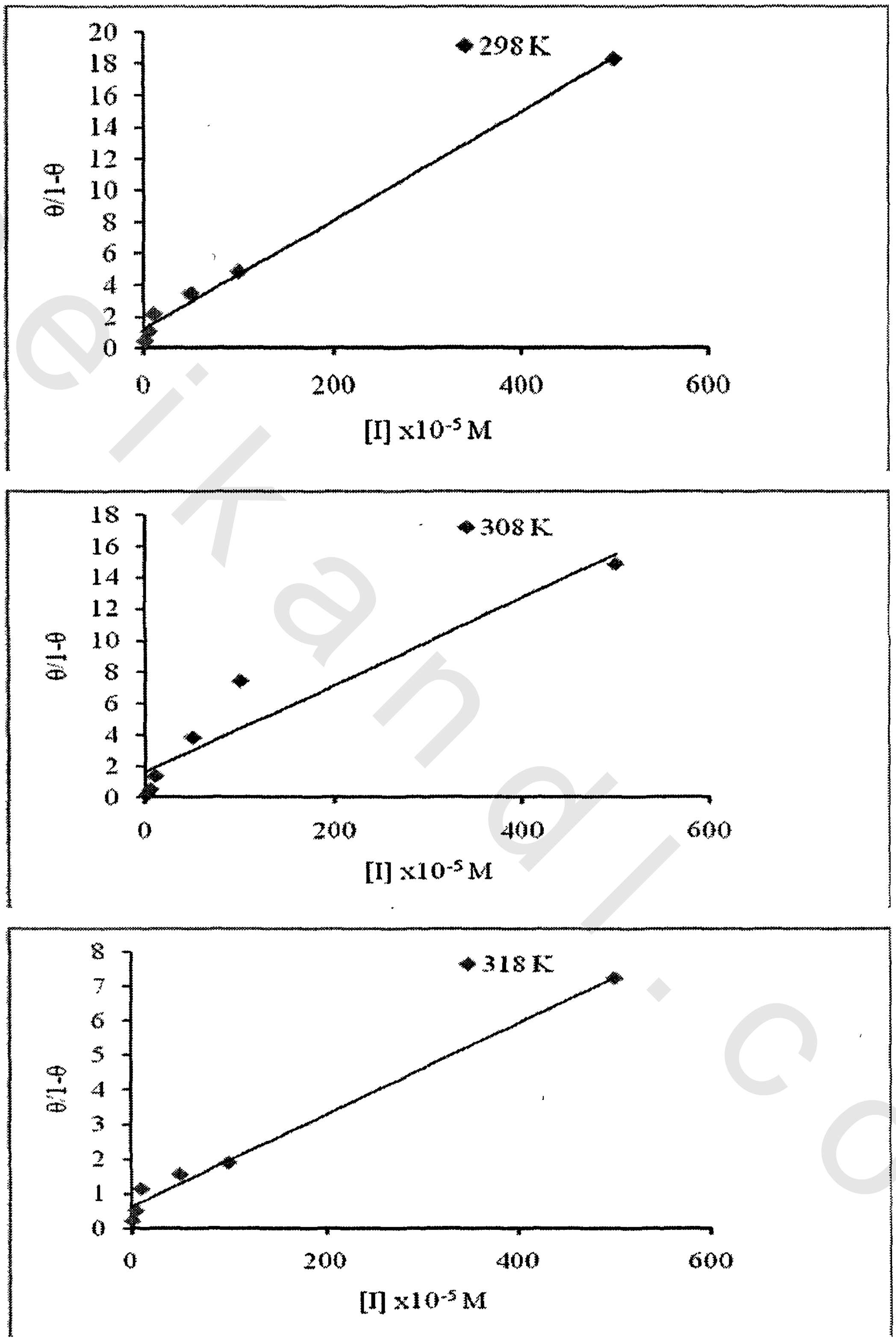

Figure (21): Relation between (θ / 1– θ) and concentration of compound (III).

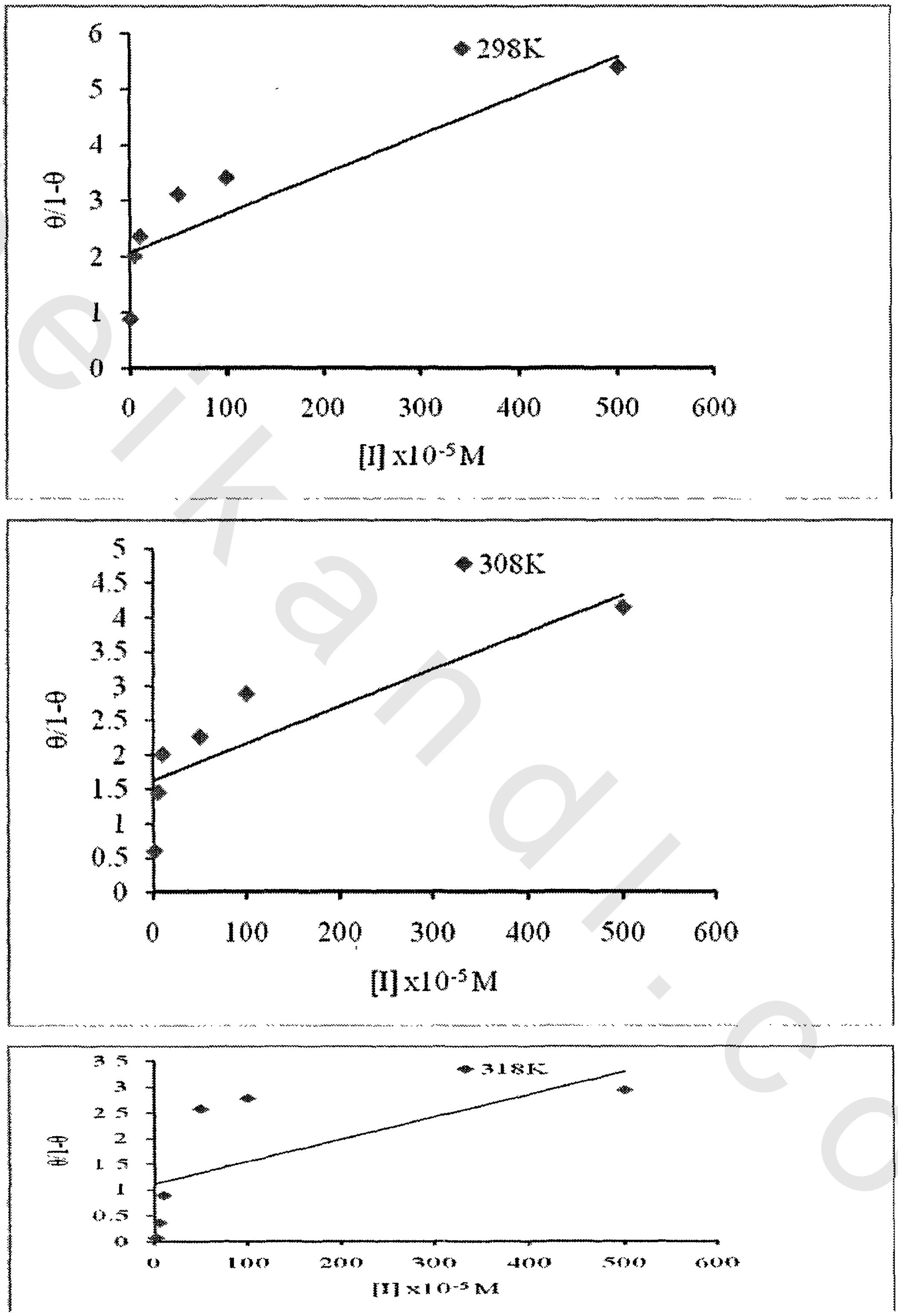

Figure (22): Relation between (θ / 1– θ) and concentration of compound (IV).

3.3.1.4 .The Thermodynamic Parameters of Adsorption:

It is generally accepted that organic molecules inhibit corrosion by adsorption at the metal–solution interface and that the adsorption depends on the molecule's chemical composition, the temperature and the electrochemical potential at the metal/solution interface [126]. The thermodynamic parameters play an important role in understanding the inhibitive mechanism. The adsorption heat could be calculated according to the Van't Hoff equation [127,128].

$$\ln K_{ads} = (-\Delta H/RT) + \text{constant} \quad (27)$$

Where ΔH and K_{ads} are the adsorption heat and adsorptive equilibrium constant, respectively.

It should be noted that $(-\Delta H/R)$ is the slope of the straight line of (lnK) against (1/T) according to equation (27):

The adsorption heat (ΔH) can be approximately regarded as the standard adsorption heat (ΔH^0) under experimental conditions [129,130].

Thus, the standard adsorption free energy (ΔG^0) could be obtained according to equation (28) [131,132]:

$$\Delta G^0 = -RT \ln K_{ads} \quad (28)$$

Then the standard adsorption entropy (ΔS^0) can be obtained by the basic thermodynamic equation (29):

$$\Delta S^0 = (\Delta H^0 - \Delta G^0)/T \quad (29)$$

The calculated thermodynamic parameters are listed in Tables (22-25). The standard adsorption heat are (-29.84,-64.84, -37.25 and-18.85 kJ mol^{-1}) for compounds (I), (II), (III), and (IV), respectively. The negative values of ΔH^0 also show that the adsorption of inhibitor is an exothermic process [133]. The negative values of ΔG^0 indicate that the adsorption of inhibitor molecule onto steel surface is a spontaneous process. Generally, values of ΔG^0 up to-20 kJ mol^{-1} are consistent with the electrostatic interaction between the charged molecules and the charged metal (physical adsorption) while those more negative than -40 kJ mol^{-1} involve sharing or transfer of electrons from the inhibitor molecules to the metal surface to form a coordinate type of bond (chemisorptions) [130-131].By inspection of data in Tables (22-25) it is obvious that the values of ΔG^0 is less than -40 kJ mol^{-1} which indicate that the adsorption is physical adsorption. Also, the negative values of ΔS^0mean that the process of adsorption is accompanied by a decrease in entropy. It might be explained as follows:

Before the adsorption of compounds onto the steel surface, the chaotic degree of steel surface is high, but when inhibitor molecules were orderly adsorbed onto the steel surface, hence the entropy decreases.

Table (22): Thermodynamic parameters of adsorption process in presence compound (I).

T (K)	ln K_{ads}	- ΔG° (kJmol^{-1})	ΔH° (kJmol^{-1})	ΔS° (J mol $^{-1}$K^{-1})
298	7.68	19.04	-29.84	-36.24
308	7.61	19.45		-33.73
318	6.92	18.29		-36.32

Table (23): Thermodynamic parameters of adsorption process in presence compound (II).

T (K)	ln K_{ads}	- ΔG° (kJmol^{-1})	ΔH° (kJmol^{-1})	ΔS° (J mol $^{-1}$K^{-1})
298	9.51	23.56	-64.48	-13.73
308	8.02	20.52		-14.27
318	7.82	20.85		--13.72

Table (24): Thermodynamic parameters of adsorption process in presence compound (III).

T (K)	ln K_{ads}	- ΔG° (kJmol^{-1})	ΔH° (kJmol^{-1})	ΔS° (J mol $^{-1}$K^{-1})
298	8.14	20.16	-37.25	-57.35
308	7.93	20.30		-55.03
318	7.19	19.00		-57.39

Table (25): Thermodynamic parameters of adsorption process in presence compound (IV).

T (K)	ln K_{ads}	- ΔG^o (kJmol^{-1})	ΔH^o (kJmol^{-1})	ΔS^o (J mol $^{-1}$K^{-1})
298	6.55	16.23	-18.85	-08.83
308	6.29	16.11		-08.92
318	6.07	16.05		-08.80

3.3.2. Tafel Polarization Measurements.

The generation of polarization curves continues to be important in aqueous corrosion research. The time-consuming potentiostatic method has been largely replaced by the potentiodynamic approach where the potential (E) of the corroding metal is automatically varied with the time. The current (i) needed to maintain the metal (working electrode) at each applied potential is ascertained and the potential/current data is plotted to give the experimental polarization curve. Extrapolation of Tafel lines is one of the most popular direct current (DC) techniques for estimation of corrosion rate. The extrapolation of anodic and/or cathodic Tafel lines for charge transfer controlled reactions give the corrosion current density, i_{corr}, at the corrosion potential, E_{corr} .

Corrosion current densities were obtained from the polarization curves by linear extrapolation of the Tafel curves. Since the corrosion rate is directly related to the corrosion current i_{corr}, the inhibition efficiency η% at different inhibitor concentrations were calculated from the equation:

$$\eta\% = \{(i_{corr} - i_{corr}^{\backslash}) / i_{corr0}\} \times 100 \quad (30)$$

Where i_{corr} and $i_{corr}^{\backslash}$ are the corrosion current densities ($mAcm^{-2}$) with and without addition of inhibitor, respectively.

The anodic and cathodic polarization curves for carbon steel in 1M H_2SO_4 at different concentrations of all prepared inhibitors are shown in Fig(26-29) It is clear that the presence of inhibitor causes a marked decrease in the corrosion rate, i.e. Shift the anodic curves to more positive potentials and the cathodic curves to more negative potentials. This may be ascribed to adsorption of inhibitor over the corroded surface [136]. The values of corrosion current densities (i_{corr}), corrosion potential (E_{corr}), the cathodic Tafel slope (bc), anodic Tafel slope (ba), and the inhibition efficiency (η %) as functions of corrosion inhibitor concentrations, were calculated from the curves of Figures (23-26) and are given in Tables (26-29).Tables (26-29) reveals that the corrosion current decreases obviously and the efficiency η % increases with the inhibitor concentration. The presence of corrosion inhibitors does not markedly shift the corrosion potential, while the anodic and cathodic Tafel slopes change upon addition of increasing inhibitor concentration. Therefore, these corrosion inhibitors can be act as mixed-type inhibitors in 1M H_2SO_4. Similar results have been reported with other organic compounds in acidic medium [137-138]. From Tables (26-29), it can be concluded that inhibition efficiencies obtained from weight loss and electrochemical polarization curves are in good agreement.

Table (26): Potentiodynamic polarization parameters of compound (I) in 1M H_2SO_4 at 298 K

Conc.x10^5 (M)	**-E$_{corr}$** (mV)	**i$_{corr}$** (mAcm^{-2})	**b$_a$** (mVdec^{-1})	**-b$_c$** (mV dec^{-1})	**η %**
0.00	522.6	0.97	115.6	200.6	0.00
1.00	499	0.38	58.3	127.4	59.7
5.00	496.4	0.29	54.2	119.9	60.8
10.0	509.7	0.15	86.6	131.0	70.1
50.0	482.8	0.12	55.7	125.3	84.5
100	526.3	0.09	71.9	179.0	87.5
500	497.7	0.05	61.9	131.1	90.7

Table (27): Potentiodynamic polarization parameters of compound (II) in 1M H_2SO_4 at 298 K

Conc.x10^5 (M)	**-E$_{corr}$** (mV)	**i$_{corr}$** (mAcm^{-2})	**b$_a$** (mVdec^{-1})	**-b$_c$** (mV dec^{-1})	**η %**
0.00	522.6	0.97	115.6	200.6	0.00
1.00	529.8	0.39	73.1	131.6	59.7
5.00	497.5	0.12	54.1	217.5	87.6
10.0	489.5	0.07	41.9	161.2	92.7
50.0	497.0	0.05	61.9	131.1	94.8
100	529.0	0.03	140.3	142	96.9
500	479.3	0.02	74.4	151.2	97.9

Table (28):Potentiodynamic polarization parameters of compound (III) in 1M H_2SO_4 at 298 K.

Conc.x10^5 (M)	-**E$_{corr}$** (mV)	**i$_{corr}$** (mAcm^{-2})	**b$_a$** (mVdec^{-1})	-**b$_c$** (mV dec^{-1})	**η %**
0.00	522.6	0.97	115.6	200.6	0.00
1.00	533.2	0.41	92.6	170.4	57.7
5.00	499.1	0.39	58.3	125.4	59.7
10.0	552.2	0.11	158.8	168.2	73.1
50.0	526.5	0.09	71.9	179.5	76.9
100	489.5	0.07	52.8	158.7	92.7
500	474.0	0.05	40.1	144.3	94.8

Table (29):Potentiodynamic polarization parameters of compound (IV) in 1M H_2SO_4 at 298 K.

Conc.x10^5 (M)	-**E$_{corr}$** (mV)	**i$_{corr}$** (mAcm^{-2})	**b$_a$** (mVdec^{-1})	-**b$_c$** (mV dec^{-1})	**η %**
0.00	522.6	0.97	115.6	200.6	0.00
1.00	519.0	0.61	100.3	192	37.1
5.00	496.0	0.30	54.2	119.9	69.0
10.0	526.1	0.18	76.5	156.2	70.4
50.0	532	0.10	70.2	157.6	89.6
100	527.0	0.09	71.9	179.0	90.7
500	489.0	0.06	40.9	146.2	93.8

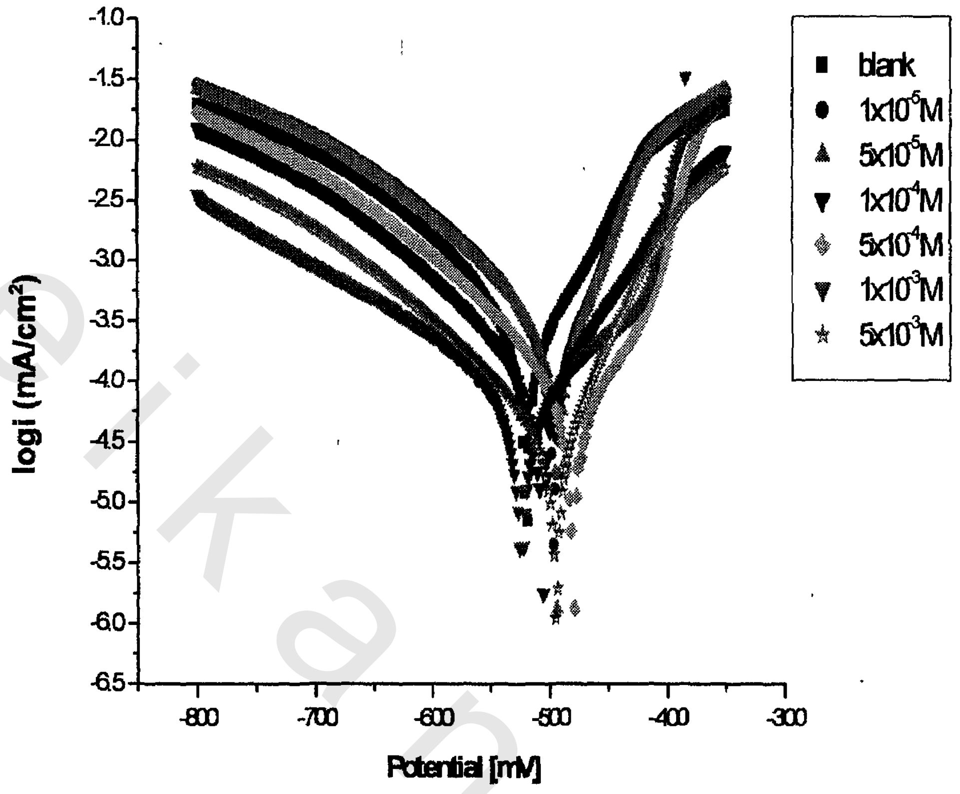

Figure (23): Tafel line for the carbon steel sample in 1 M H_2SO_4 in absence and presence different concentrations of compound I at 298 K.

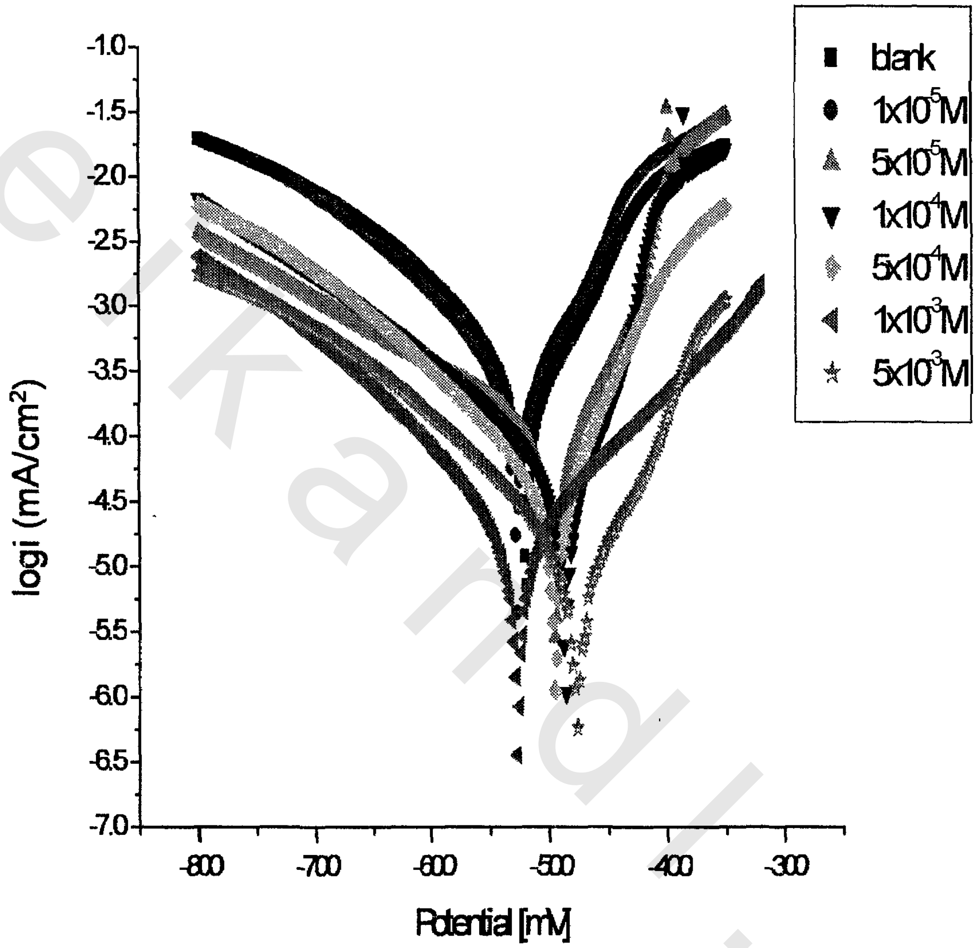

Figure (24): Tafel line for the carbon steel sample in 1 M H_2SO_4 a in absence and presence different concentrations of compound II at 298 K.

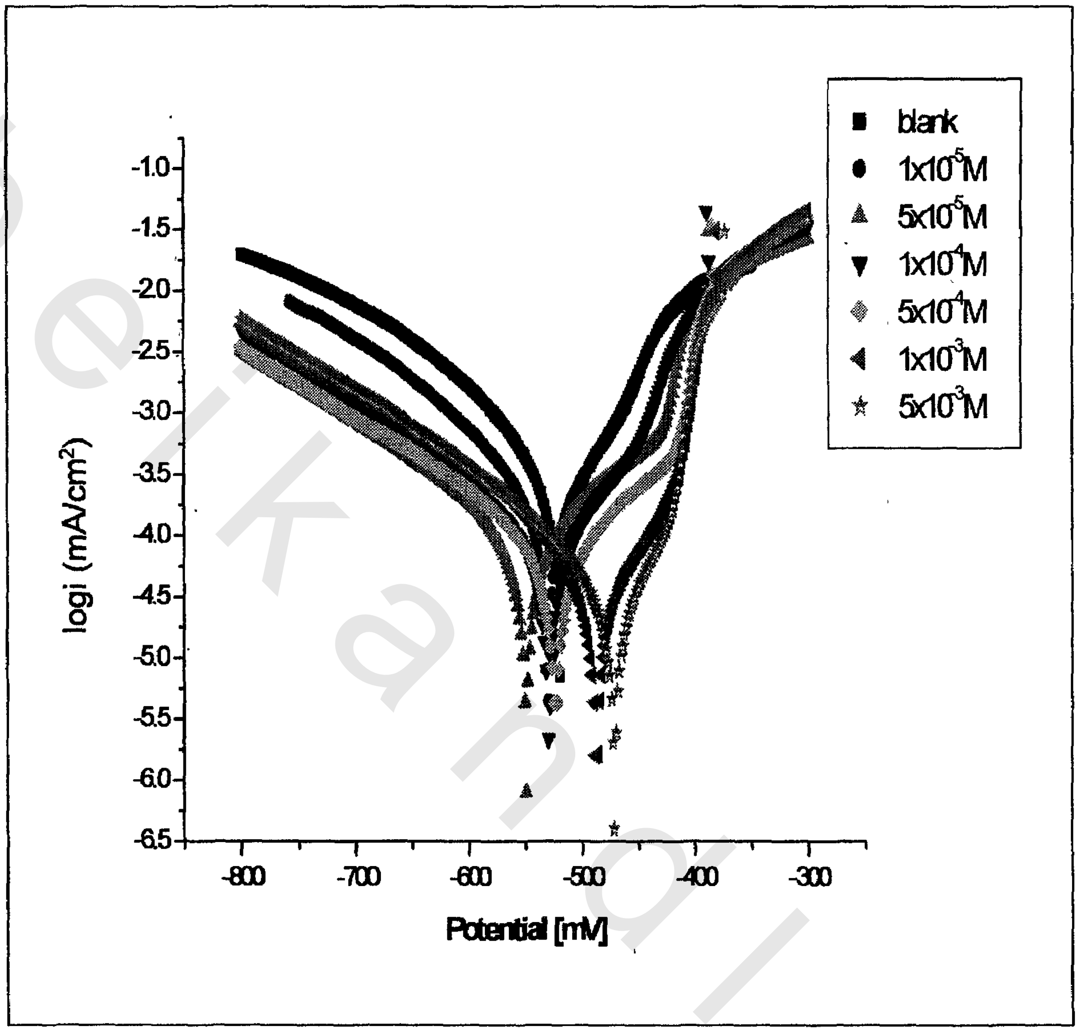

Figure (25): Tafel line for the carbon steel sample in 1 M H_2SO_4 in absence and presence different concentrations of compound III at 298 K .

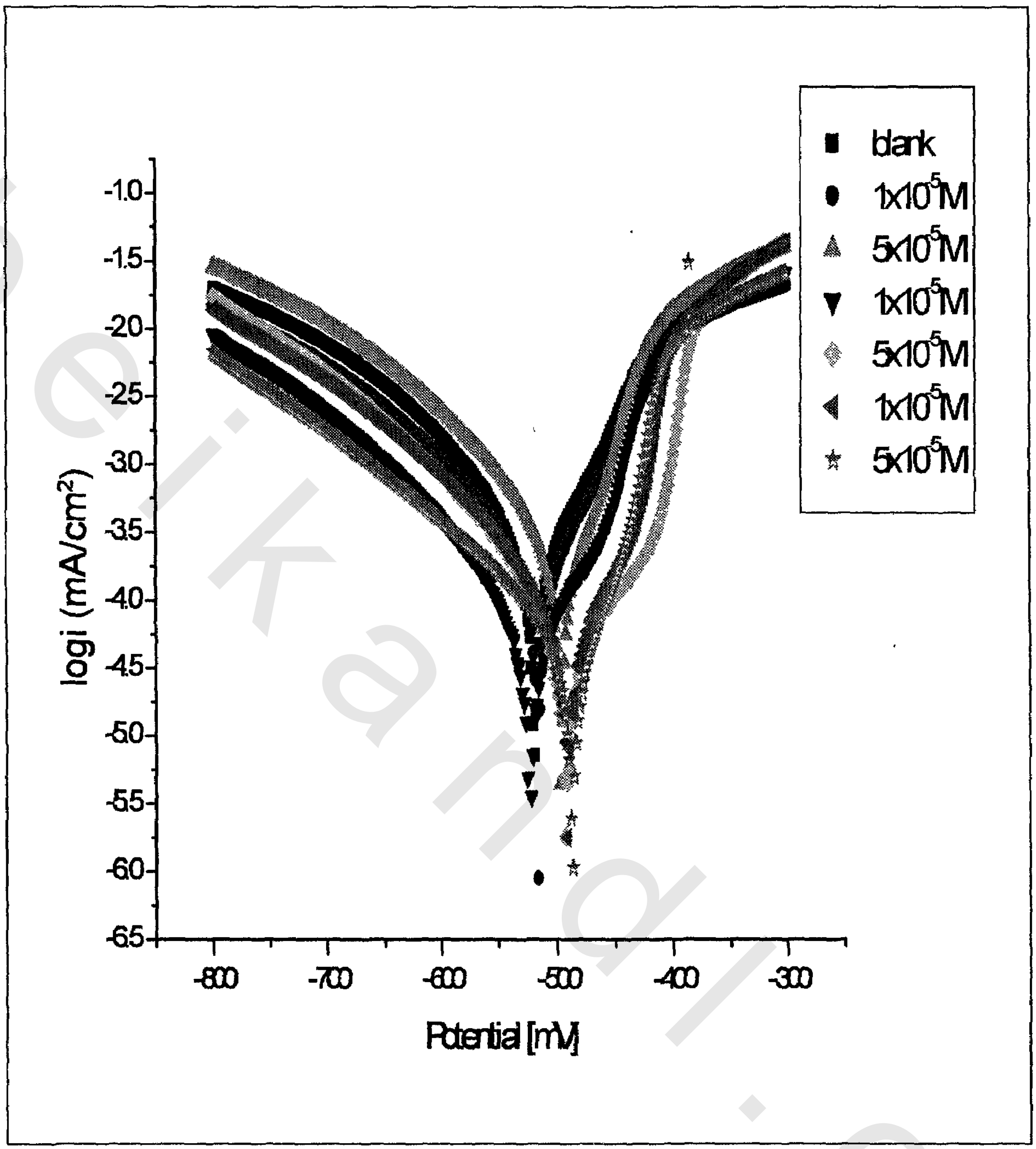

Figure (26): Tafel line for the carbon steel sample in 1 M H_2SO_4 in absence and presence different concentrations of compound IV at 298 K.

3.3.3 . Impedance Measurements.

Electrochemical Impedance Spectroscopy (EIS) has many advantages in comparison with other electrochemical techniques. During EIS experiments, a small amplitude alternating current (AC) signal is applied to the system being studied. Therefore, it is a non-destructive method for the evaluation of a wide range of materials, including coatings, anodized films and corrosion inhibitors.

Figures (27-28) show the impedance diagrams (Nyquist plots) for the working electrode immersed in the corrosive media (1 M H_2SO_4) in the absence and in presence of different concentrations of the prepared compounds (I–II), respectively, at a temperature of 298 K . These impedance diagrams are not perfect semicircles which have been attributed to frequency dispersion [139-140]. The charge transfer resistance (R_t) values were calculated from the difference in impedance at lower and higher frequencies, as previously suggested [141]. These R_t values are listed in Tables (32.33) for the prepared inhibitors (I–II), respectively. The double layer capacitance, C_{dl}, was determined from frequency, f, at which Zi was maximum, using the relationship.

$$f\,(-Z_{max}) = (2\pi C_{dl}\,R_t)^{-1} \qquad (31)$$

The inhibition efficiency, η%, of the working electrode is calculated from the charge transfer resistance, R_t, using the equation:

$$\eta\% = \{(R_t^{\backslash} - R_t)/R_t^{\backslash}\}\ x100 \qquad (32)$$

Where $R_t^{\backslash}$ is the charge-transfer resistance in the inhibited solutions and R_t in the uninhibited solution , The impedance parameters derived from these investigations are given in tables

(30-31) the results of this table indicate that as surfactant concentration increases the values of Rt and η % increase, but the values of C_{dl} decrease. This indicates the occurrence of adsorption of surfactants on the electrode surface.

Table (30): Impedance parameters of carbon steel in 1 M H_2SO_4 in presence of different concentrations compound (I) at298 K.

Conc.x10^5 M	R_t(Ω.cm^2)	C_{dl}(μFcm^{-2})	η%
0.00	094.39	226.40	00.00
1.00	162.88	189.30	42.05
5.00	206.02	165.10	54.18
10.0	322.84	85.90	60.83
50.0	340.99	76.09	70.76
100	404.88	75.87	76.69
500	482.84	68.87	80.45

Table (31): Impedance parameters of carbon steel in 1 M H_2SO_4 in presence of different concentrations compound (II)at 298 K.

Conc.x10^5 M	R_t(Ω.cm^2)	C_{dl}(μFcm^{-2})	η%
0.00	094.39	226.40	00.00
1.00	151.42	176.80	37.66
5.00	208.19	99.85	54.66
10.0	412.12	85.90	77.10
50.0	551.49	56.74	82.81
100	549.25	51.41	82.88
500	768.23	48.83	87.71

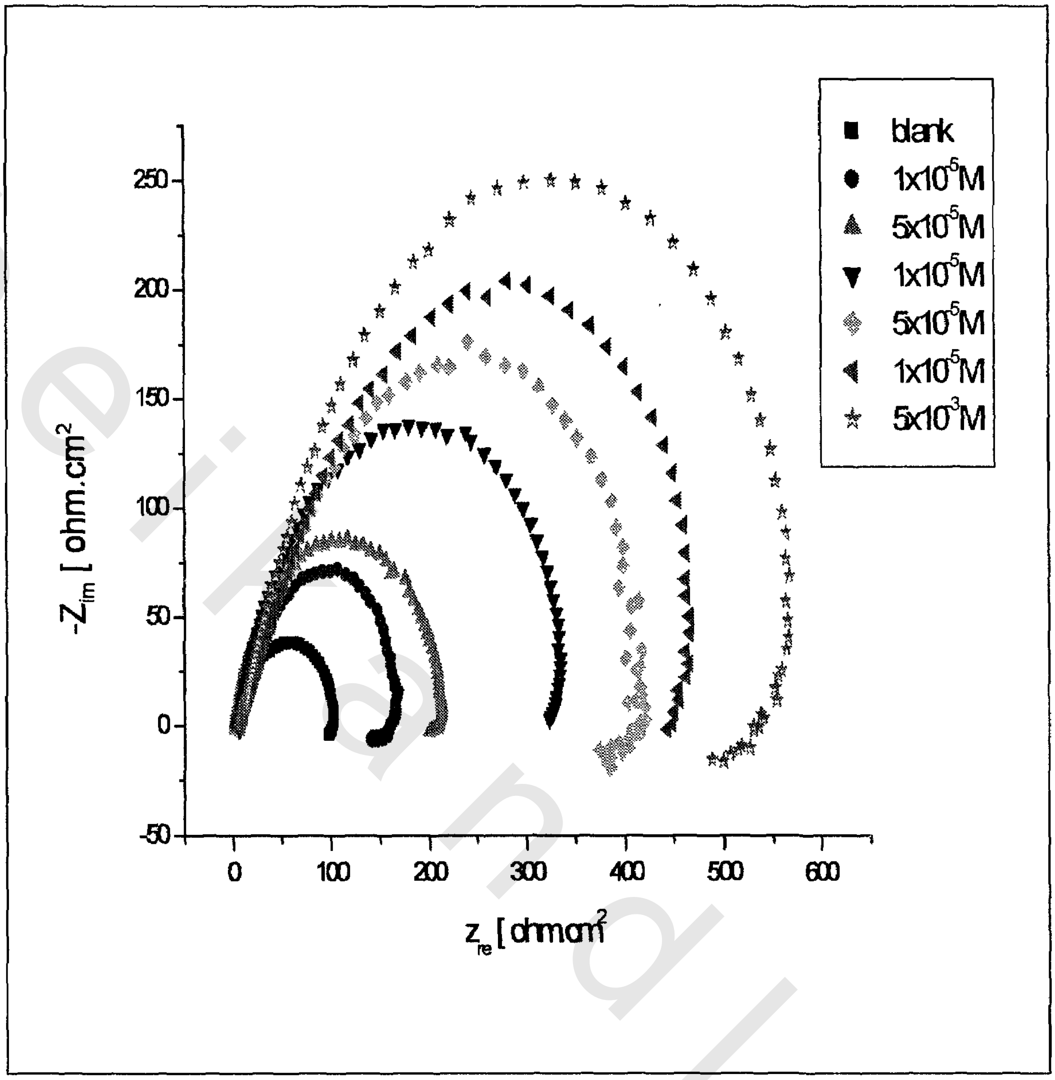

Figure (27) Nyquist plots for carbon steel in 1 M H_2SO_4 in absence and presence of different concentrations of compound I at 298 K.

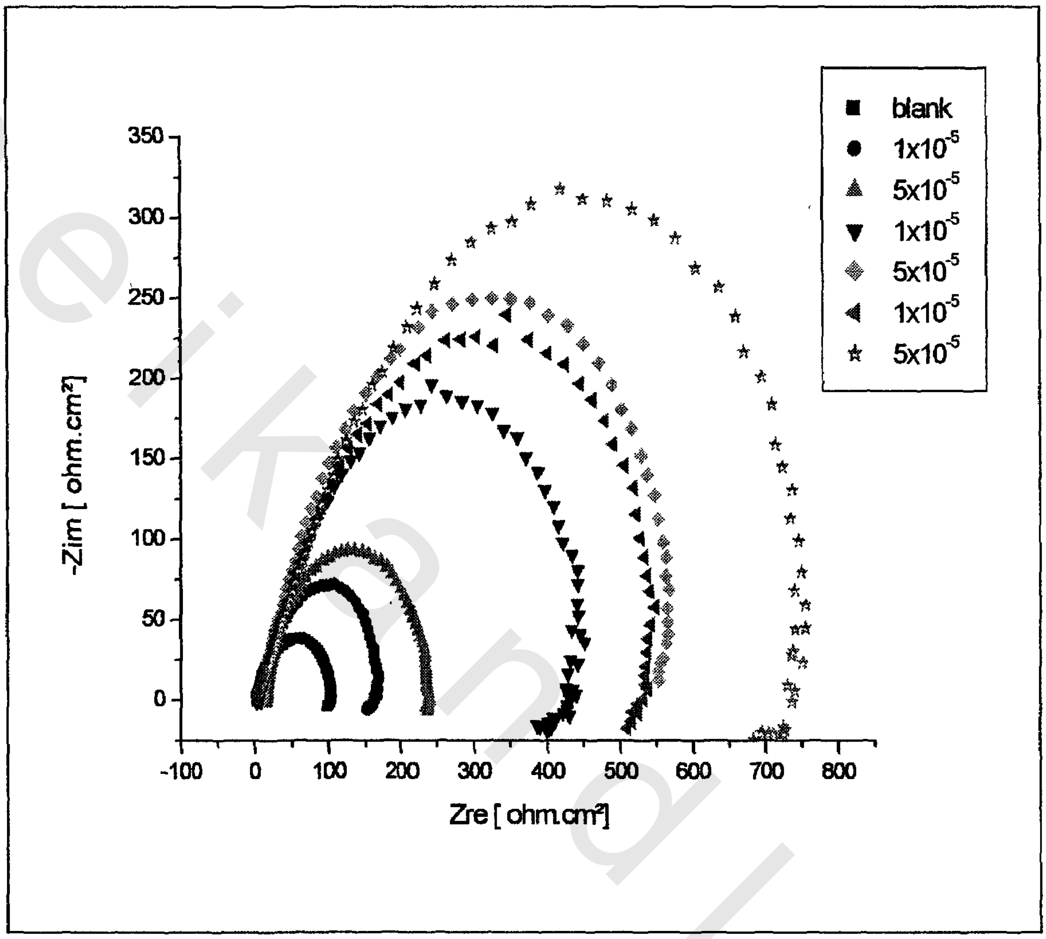

Figure (28) Nyquist plots for carbon steel in 1 M H_2SO_4 in absence and presence of different concentrations of compound II at298 (K).

3.4. Antimicrobial Activity:

The biocidal effect of any cationic surfactants may due to the following:

1. Inhibit cell wall synthesis
2. Injuring the cytoplasmic membrane
3. Inhibiting protein biosynthesis
4. Inhibiting nucleic acid synthesis

It has been recognized from previous research, the cationic surfactants have antibacterial activity [142-145]. Investigations of structure-activity relationships have demonstrated that in addition to a cationic site, a significant lipophilic part of the surfactant is involved in optimization of activity. A series of the prepared quaternary ammonium salts containing hydrophobic chains of varying length were tested against some pathogenic Gram-positive (Staphylococcus aureus and Bacillus subtilis) and Gram-negative (Escherichia coli and Desulfomonas pigra) bacteria and also, some pathogenic fungi (Candida albicans and Asperigllus flavus).

The antimicrobial activity results of the synthesized cationic surfactants against pathogenic bacteria and fungi are recorded in Table (32) indicating that the synthesized (QATS) have good antimicrobial activity and the difference in its activity related to the length of hydrophobic chains and interfacial properties of the prepared surfactants. The optimal length of the alkyl chain has been noted to be ten carbon atoms, which have the maximum inhibition zone. These results are in good agreement with results obtained before, which indicate that the optimal activity toward a variety which alkyl chain which between ten and fourteen carbon atoms is present [146-1150].

The mode action of such cationic surfactants on bacteria is understood to be one of electrostatic interaction and physical disruption, as opposed to interference with a metabolic pathway, as is commonly the situation with antibiotic species. After the cationic site of the surfactant attached to a significant lipophilic component binds to anionic sites of the cell wall surface it is then able to diffuse through the cell wall and bind to the membrane. Acting as a surfactant, it is able to disrupt the membrane and permit the release of electrolytes and nucleic materials, leading to cell death. The membrane activity of the surfactants depends on the character of the polar head groups (size and electric charge distribution) and hydrocarbon chains (length, saturation and multiple chains).

Table (32): Antimicrobial activity of the synthesized surfactants against pathogenic bacteria and fungi.

compound	Inhibition zone diameter, (mm/mg sample)				
	Esherichi Ecoli (G^-)	Staphylococcus aireus (G^+)	Aspergillus flavs (Fungus)	Candida albicans (Fungus)	Desulfomonas pigar SRB
I	43	44	40	25	42
II	40	41	31	21	22
III	21	23	16	17	17
IV	15	18	14	13	14